ESTIMATION OF THE ENERGY OUTPUT OF A PHOTOVOLTAIC PANEL BY METAHEURISTIC OPTIMIZATION BASED ARTIFICIAL NEURAL NETWORKS

2022
MASTER THESIS
MECHATRONICS ENGINEERING

Ali Kamil Gumar GUMAR

Assist.Prof.Dr. Funda DEMİR

ESTIMATION OF THE ENERGY OUTPUT OF A PHOTOVOLTAIC PANEL BY METAHEURISTIC OPTIMIZATION BASED ARTIFICIAL NEURAL NETWORKS

Ali Kamil Gumar GUMAR

T.C.
Karabuk University
Institute of Graduate Programs
Department of Mechatronics Engineering
Prepared as
Master Thesis

Assist.Prof.Dr. Funda DEMİR

KARABUK
November 2022

I certify that in my opinion the thesis submitted by Ali Kamil Gumar GUMAR titled "ESTIMATION OF THE ENERGY OUTPUT OF A PHOTOVOLTAIC PANEL BY METAHEURISTIC OPTIMIZATION BASED ARTIFICIAL NEURAL NETWORKS" is fully adequate in scope and in quality as a thesis for the degree of Master of Science.

Assist.Prof.Dr. Funda DEMİR .....
Thesis Advisor, Department of Mechatronics Engineering

This thesis is accepted by the examining committee with a unanimous vote in the Department of Mechatronics Engineering as a Master of Science thesis. November 25, 2022

Examining Committee Members (Institutions)	Signature
Chairman : Assoc.Prof.Dr. Serhat Orkun TAN (KBU)	.....
Member : Assoc.Prof.Dr. Aytaç ALTAN (BEUN)	.....
Member : Assist.Prof.Dr. Funda DEMİR (KBU)	.....

The degree of Master of Science by the thesis submitted is approved by the Administrative Board of the Institute of Graduate Programs, Karabük University.

Assoc.Prof.Dr. Müslüm KUZU .....
Director of the Institute of Graduate Programs

"I declare that all the information within this thesis has been gathered and presented in accordance with academic regulations and ethical principles and I have according to the requirements of these regulations and principles cited all those which do not originate in this work as well."

Ali Kamil Gumar GUMAR

ABSTRACT

M.Sc. Thesis

ESTIMATION OF THE ENERGY OUTPUT OF A PHOTOVOLTAIC PANEL BY METAHEURISTIC OPTIMIZATION BASED ARTIFICIAL NEURAL NETWORKS

Ali Kamil Gumar GUMAR

Karabük University
Faculty of Engineering
Department of Mechatronics Engineering

Thesis Advisor:
Assist. Prof. Dr. Funda Demir
November 2022, 71 pages

Photovoltaic (PV) solar energy has become the most prominent concern of global investments. In addition, it is considered low carbon and its manufacture has a lower carbon impact compared to other energy sources. It is one of the solutions to avoid the risks of climate and global warming and to serve the consumer. Accurate forecasting of photovoltaic power output is very important in terms of panel installation, energy management and distribution, system reliability and integrating it into the daily demand schedule of electrical power supply networks. It is necessary to create a prediction model of photovoltaic energy that is commensurate with the changing weather conditions to develop advanced technology. Our study aims to develop a new data acquisition system dedicated to photovoltaic systems, meteorological observations and prediction of solar energy outputs. We use micro-controllers and sensors for barometer measurements. Weather and

electrical balances are archived on our websites and monitored through the Internet of Things via the thinkspeak platform. The Artificial Neural Networks (ANN) model which was improved by metaheuristic algorithms was used to predict the solar energy outputs collected during 37 days from Monday May 9, 2022 to Wednesday June 15, 2022. Three main algorithms, Genetic Algorithm (GA), Particle Swarm Optimization (PSO) and Artificial Bee Colony (ABC) were used to train ANN to predict an 18-degree solar panel. They used three common methods to evaluate and compare the results of the algorithms used which are mean square error (MSE), mean absolute percentage error (MAPE) and coefficient of determination (R^2). The results show that traditional NN with basic finding methods is the best. PSO-ANN is the best between PSO-ANN, GA-ANN and ABC-ANN.

Key Word : **A**rtificial neural network (ANN); artificial bee colony (ABC); genetic algorithm (GA); particle swarm optimization (PSO); solar photovoltaic (PV); PV power production forecasting; Internet of Things (IoT) in PV systems; online systems monitoring.

Science Cod : 92906

ÖZET

Yüksek Lisans Tezi

BİR FOTOVOLTAİK PANELİN ENERJİ ÇIKIŞININ METAHEURİSTİK OPTİMİZASYON TABANLI YAPAY SİNİR AĞLARI İLE TAHMİNİ

Ali Kamil Gumar GUMAR

Karabük Üniversitesi
Fen Bilimleri Enstitüsü
Mekatronik Mühendisliği Anabilim Dalı

Tez Danışmanı:
Dr. Öğr. Üyesi Funda Demir
Kasım 2022, 71 sayfa

Fotovoltaik (PV) güneş enerjisi, küresel yatırımların en önemli endişesi haline gelmiştir. Bunu yanı sıra, diğer enerji kaynaklarına kıyasla daha düşük karbon etkisine sahiptir. İklim ve küresel ısınma risklerinden korunmak ve bu anlamda tüketiciye hizmet etmek için kullanılan çözüm yollarından biridir. Fotovoltaik güç çıkışının doğru tahmini, panel kurulumu, enerji yönetimi ve dağıtımı, sistem güvenilirliği ve elektrik güç kaynağı şebekelerinin günlük talep çizelgesine entegre edilmesi açısından çok önemlidir. Bu nedenle, ileri teknoloji geliştirmek için değişen hava koşulları ile orantılı bir fotovoltaik enerji tahmin modelinin oluşturmak gerekir. Gerçekleştirilen çalışmada fotovoltaik sistemlere, meteorolojik gözlemlere ve güneş enerjisi çıktılarının tahminine yönelik yeni bir veri toplama sistemi geliştirmek amaçlanmaktadır. Barometre ölçümleri için mikro denetleyiciler ve sensörler kullanılmaktadır. Hava durumu ve elektrik dengeleri web sitesinde arşivlenmekte ve Thinkspeak platformu aracılığıyla Nesnelerin İnterneti üzerinden izlenmektedir.

9 Mayıs 2022 Pazartesi ile 15 Haziran 2022 Çarşamba arasındaki 37 gün boyunca toplanan güneş enerjisi çıktılarını tahmin etmek için metasezgisel algoritmalarla geliştirilmiş Yapay Sinir Ağları (YSA) modeli kullanılmıştır. Üç ana algoritma, Genetik Algoritma (GA), Parçacık Sürü Optimizasyonu (PSO) ve Yapay Arı Kolonisi (ABC), 18 derecelik eğim ile yerleştirilmiş güneş paneline ait verileri tahmin etmek için kullanılmıştır. Bu algoritmaların sonuçlarını değerlendirmek ve karşılaştırmak için ortalama kare hatası (MSE), ortalama mutlak yüzde hatası (MAPE) ve belirleyicilik katsayısı (R^2) olmak üzere üç yöntem kullanılmıştır. Sonuçlar, temel belirleme yöntemlerini kullanan geleneksel yapay zeka yönteminin en iyisi olduğunu göstermektedir. PSO-ANN ise GA-ANN ve ABC-ANN ile karşılaştırıldığında en iyi sonucu vermektedir.

Anahtar Sözcükler : Yapay sinir ağı (YSA); yapay arı kolonisi (ABC); genetik algoritma (GA); parçacık sürüsü optimizasyonu (PSO); güneş fotovoltaik (PV); PV güç üretimi tahmini; PV sistemlerinde Nesnelerin İnterneti (IoT); çevrimiçi sistem izleme.

Bilim Kodu **:** 92906

ACKNOWLEDGMENT

May God’s Blessings Be Upon Mohammed and His Pure Immediate Family.

"My Lord, direct me to be thankful for the blessings you have bestowed upon me and upon my parents, and to do good works that please You".

(An-Naml : 19)

I thank God Almighty first and foremost for the great grace that He has bestowed upon me and gave me strength, patience, and the ability to overcome difficulties and complete this thesis then I thank those who favored them. My beloved parents the source of love, mercy and tenderness do not cease to me for all their efforts from the moment of my birth to these blessed moments. Your prayers lightened and eased the way for me to complete my study. Hope this achievement make you proud of me.

I extend my sincere thanks and gratitude to my brothers and sisters for their continuous support and encouragement, which had a great impact in overcoming obstacles and difficulties.

I extend my thanks, appreciation and gratitude to the virtuous professor Assist. Prof. Dr. Funda Demir. I was pleased with her supervision of this thesis, and his constructive guidance, good spirit and generous character had a great impact on the completion of this thesis.

And I especially thank the distinguished professor: Assist. Prof. Dr. Batikan Demir, for his technical support and guidance throughout the preparation and construction of the experimental setup measuring system and for guiding me with advice education and correction.

CONTENTS

Page

Page

Page

LIST OF FIGURES

Page

Page

LIST OF TABLES

Page

SYMBOLS AND ABBREVITIONS INDEX

SYMBOLS

$Pf\ t\ +\ h$	: expected power output
$Ppd\ (t)$	: power output
x(t)	: represents the forecasted PV power
p, q	: indicate the order
αi	: AR models coefficients
β_j	*:* MA models coefficients
e(t)	: white noise
U_N	: final network output
w_j	: connection weight
I_j	: input number
b	: bias weight
N	: several inputs
x	: vectors input space
x_i	: vector of features computed
E	: output voltage
S	: sensitivity of the pyranometer
I	: solar irradiance
$f(\boldsymbol{x})$	: minimizes cost function
$\boldsymbol{x}$	: one dimension
$\boldsymbol{S}$	: which its dimensional
l_i	: variable domains are limited by lower bounds
u_i	: variable domains are limited by upper bounds
$p = 0$	: unconstrained optimization problem
$q = 0$	: unconstrained optimization problem

x_{mi} : neighborhood of the food source

x_{ki} : randomly selected food source

i : randomly chosen parameter index

ϕ_{mi} : random number within the range $[-a, a]$

υ_m : fitness is calculated

$F_m(x_m)$: fitness value of the solution

p_m : onlooker bee phase

$\boldsymbol{Y}$: vector of real values

$\widehat{\mathbf{Y}}$: predicted values of

N : length of vectors

ABBREVITIONS

PV : Photovoltaic

LCOE : Levelized Cost of Electricity

IEA : International Energy Agency

MPPT : Maximum Power Point Tracking

ML : Machine Learning

IoT : Internet of Things

RMSE : Root Mean Square Error

MAPE : Mean Absolute Percentage Error

R^2 : Coefficient of determination

ANN : Artificial Neural Network

SVM : Support Vector Machines

ELM : Extreme Learning Machines

FA : Firefly Algorithm

GSO : Glowworm Swarm Optimization

GRO : Group Search Optimization

PSO : Particle Swarm Optimization

GA : Genetic Algorithm

ABC : Artificial Bee Colony

NWPs : Numerical Weather Predictions

AR : Autoregressive
MA : Moving Average
ARMA : Autoregressive Moving Average
ARIMA : Autoregressive Integral Moving Average
ARMAX : Autoregressive Moving Average with Exogenous Inputs
RBFNN : Radial Basis Function Neural Network
MAD : Mean Absolute Deviation
RSM : Response Surface Method
MARS : Multivariate Adaptive Regressions
M5 Tree : M5 model tree
PFLRM : Partially Functional Linear Regression Model
MLR : Multiple Linear Regression
MLANN : Multi-Layer Artificial Neural Networks
ANR : Articulated Neural Rendering
FFNNs : Feedforward Neural Networks
MLFFNN : Multilayer Feedforward Neural Network
PVGIS : Photovoltaic Geographical Information System
MLFFBP : Multi-Layer Feed-Forward Back-Propagation
RNN : Recurrent Neural Networks
LSTM : Long Short-Term Memory
GRU : Gates Repeated Unit
NRMSE : Normalized Root Mean Squared Error
ME : Mean Error
MSE : Mean Squared Error
MAE : Mean Absolute Error
NAR : Nonlinear autoregressive
LSSVM : Least-Squares Support-Vector Machines
ANFIS : Adaptive Network-Based Fuzzy Inference System
LMA : Levenberg–Marquardt Algorithm
SLFN : Single-hidden Layer Feedforward Network
KNN : K- Nearest Neighbor
RF : Random Forest
ACO : Ant Colony Optimization

BPNN : Back Propagation Neural Network

APSO : Accelerate Particle Swarm Optimization

CRPSO : Craziness PSO

BPFFANN : Back Propagation Feed Forward Artificial Neural Network

PWM : Pulse Width Modulation

I2C : Inter-Integrated Circuit

I2S : Inter-IC Sound

SMBus : System Management Bus

ADC : Analog-to-Digital Converter

DAC : Digital -to- Analog Converter

GPIO : General-Purpose Input/Output

SPI : Serial Peripheral Interface

UART : Universal Asynchronous Receiver-Transmitter

BLE : Bluetooth Low Energy

BR/EDR : Basic Rate/Enhanced Data Rate

RSS: : Residual Sum of Squares

TSS : Total Sum of Squares

NMSE : Normalized Mean Square Error

SECTION 1

INTRODUCTION

The development of any country going to depend primarily on energy generation, consumption, and secure storing. The development of technology and the expansion of industry have increased our need on energy. Fossil fuels are the main source of electricity, and they primarily and directly damage the environment [1]. The melting of glaciers, the rise of sea levels, and the drying out of agricultural regions are all consequences of global warming, which is caused by the combustion of fossil fuels. The demand for energy by the population all over the world is at the highest rate than ever before, causes an increase in the rate of fossil fuel combustion, leads to global warming a changing in the environment worldwide and energy resources are getting more scarce [2]. To satisfy the rising global energy demand, environmentalists and economists support climate accords and switch to cleaner energy that is more environmentally friendly, less expensive, and more effective. Clean energy, which includes wind power and solar photovoltaic (PV) electricity, among many other renewables, is a cheap form of energy for the global energy market. There has been a lot of buzz about Solar PV lately because they can convert solar power into useful electrical energy. Due to the fact that it gives the world's energy market access to a free fuel source, solar PV energy has emerged as the most important global issue and thus improves the medium- and long-term levelized cost of electricity (LCOE), in addition, bank green is considered low carbon and its manufacture has a lower carbon impact compared to other energy sources. It is one of the ways to reduce climate change and global warming threats while also benefiting consumers [3]. Solar energy is 516 times more abundant than oil and 157 times more than coal [4]. The COVID-19 pandemic caused many effects on the industrial sectors, especially in the solar energy sector, which was primarily affected by the spread of COVID-19 [5]–[9]. The year 2020 was considered a year of decline for the first time since 1980 and when revising expectations, it was 121-152 gigawatts for the year 2020, decreased by 8% to

become 108-143 gigawatts due to the outbreak of the epidemic [10]. And losses amounting to 1,700 megawatts which is enough to supply 288,000 homes with energy and about 3.2 billion dollars in the economic investment sector. In the first quarter of 2020, the price increased from 0.228 to 0.27 dollars/watt in the second quarter of 2020 [10], [11]. In order to lessen these detrimental impacts on the solar energy sector, governments must encourage investments and offer the appropriate incentives. It also urged certain governments to acknowledge the importance of solar energy outside of the grid [12]. On the one hand, expectations also indicate that the trend is not going in this way and predict that by 2025, solar energy will be the least expensive source of electricity [13]. Increased sales of digital applications that urged sustainable energy development organizations to raise awareness about solar energy and businesses started to provide data with ease of sales, planning, and follow-up to users through various digital channels are two positive effects of the epidemic in the solar energy sector [8]. Additions are becoming exceptionally large in the new normal in 2020 with 270 GW commissioned in 2021 and 280 GW in 2022. Annual solar additions reached 162 by 2022 which is 50% higher than the pre-coronavirus level in 2019 [14]. With Increasing continuous additions, the global capacity of solar PV energy could grow by 22% to become approximately 260 gigawatts in the year 2026 and it is expected that the global installed storage capacity will expand by about 56% to reach 270 gigawatts. This is due to the increasing need for energy and the flexibility of the storage system around the world [15]. Despite all the successes and benefits mentioned previously, the PV system was disadvantage due to the instability and regulation of the variable electric power generation when connected with the electrical network and this makes the schedule of processing and production very difficult [16]. When PV energy is widely integrated with electrical supply and distribution networks, meteorological conditions, which are the primary factor determining the generation of PV energy, enjoy a significant deal of unpredictability. As a result, precise and trustworthy solar PV forecasting is crucial to the PV power system's safe and cost-effective functioning. Based on previous weather data and solar panel PV characteristics, a specific approach is applied [17].

The development of prediction parameters for the design and installation of PV systems, such as solar radiation intensity, panel temperature, dust, wind, humidity, and ambient temperature, has been a focus of increased study due to the extensive forecast

rates in the area of solar PV systems. It was discovered that the solar panel's surface temperature rises as a result of the dust that is present there [18]. Since semiconductors are used in the production of PV electricity, the temperature has a major effect on the output voltage and current produced by the semiconductor, hence reducing the performance of the system. According to a research by Virtuani et al., the open-circuit voltage output declined by 0.45%, the rate of power production decreased by 0.65%, and the fill factor of the system reduced by 0.2% with each Kelvin increase in temperature [19], [20]. In a study done by Bahaidarah et al., when the temperature is lowered by 20% due to cooling, a solar panel's output increases by 9% [21]. Most solar panel manufacturers design their systems under hypothetical environments with cell temperatures of 25 °C, solar radiation of 1000 W/m2, and air pressure of 1.5 atm. the production of power of PV systems may explained depending on the variation of external environmental parameters [22]. During the manufacturing process of Solar panels, flaws and abnormalities may appear, causing solar panels to function less efficiently and produce less energy. Component difficulties, especially inside this DC portion (PV modules and Maximum power point tracking (MPPT)) have lowered PV productivity according to a report from the International Energy Agency (IEA). efects such as cell cracks, debonding, hot surfaces, and dirt buildup, Common PV array flaws include mismatched modules, shorted modules, poor connections, corroded connections, open circuit-short circuit faults, and MPPT failures [23]. Incorporating PV system output predictions daily data analysis and presentation demand schedule gives operators a strategy for electricity grids and system dependability [24]. Studies found that the extremely short, medium, and long periods used to categorize the energy projections for the PV system [25]. A very short time period is less than four hours, a short time period is one to three days, a medium time period is one week, and a long time period is months. A short prediction plays a critical role in predicting energy distribution over such four timeframes [26]–[28]. As a result, forecasting has a long-term focus, relies on the gathering of past data, and is based on statistical techniques [29]. In order to develop more advanced technology, it is required to establish a forecast model for photovoltaic energy that is appropriate with the various weather circumstances [30]. A lot of research has been done by scientists on the method of forecasting and optimization of renewable energy supply systems and how to solve the problems of uncertainty and prediction accuracy. Several different types of prediction

models, including persistence models, physical models, statistical models, machine learning (ML) models, metaheuristic models, and hybrid models made up of two or more models, were found after a thorough analysis of the literature. A particular emphasis was placed on the hybrid machine learning and metaheuristic models, which were examined and critically contrasted with other models and it was found that the hybrid models with optimization algorithms are the best for prediction, and it was clear through the analysis of the values for performance criteria MSE, MAPE and R^2 which decreases by about 15% compared to other models such as artificial intelligence and other specific models. Combining a few optimization techniques, such as Group Search Optimization (GRO), Firefly algorithm (FA), and Glowworm Swarm Optimization, (GSO) with ANN, Support Vector Machines (SVM), and Extreme Learning Machines (ELM) are the most often used approaches in hybrid models. Finding the optimum answers for hybrid approaches is one of these optimization algorithms' main tasks. Input data that are reliable and closely connected to solar energy output are also necessary for successful prediction.

There are two primary sections to the thesis study. Creating the measurement setup is the first step in measuring the "solar radiation level," "the current, voltage, and power output of the PV panel, battery, and load," "the temperature of the solar panel surface, ambient air, and battery," and "the humidity and pressure of the environment" in which the panel is situated. Thanks to the Internet of Things (IoT) and smart gadgets, these measures may be tracked and recorded locally or online from anywhere in the globe. Data management and power output estimation make up the second section. In this section, research is done utilizing the ANN model and optimization methods to forecast and maximize the power production of a PV system.

We will work on the data that we have quoted from the first part, and the work steps are as follows:

1. Training an ANN using MATLAB ANN-TOOL.
2. ANN Estimation Optimization by Using Optimization Algorithms like PSO, GA and ABC.
3. Comparing the results of optimization algorithms with three different common evaluation methods called MAPE, RMSE and R^2 used to make the comparison.

SECTION 2

LITERATURE REVIEW

In this part, we will present a literature review of modern renewable energy forecasting methodologies.

We will discuss and analyze different forecasting methodologies. Successful integrations of renewable energy sources into small grids need to build a reliable and accurate prediction model for solar energy and understand the random behaviours of renewable energy.

This is what we must do as engineers to choose the accurate and appropriate approach to predicting renewable energy, especially solar energy. Reliable renewable energy is one of the most prominent concerns in literary studies. Numerous studies have been done so far that focus on the flaws and errors in solar energy forecast models.

These models may be divided into several categories, including physical models, statistical models, AI models, metaheuristic models, and hybrid models, which combine two or more of the preceding models. Recently, researchers' attention has been drawn to artificial intelligence models among these prediction models, particularly machine learning with metaheuristics, which is represented by a hybrid model. In our literature review, we will concentrate on these models.

Figure 2.1 displays the uses of the electrical sector and the variations in the horizons of those uses [31].

Researchers have multiple perspectives and different ways of forecasting renewable energy sources (mainly solar energy) that will be reviewed in the following sections.

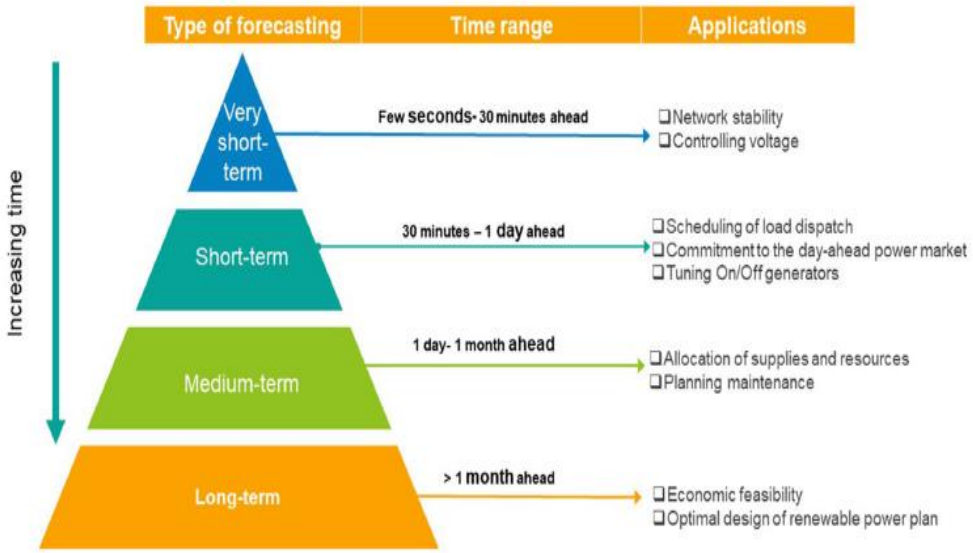

Figure 2.1. Forecasting time horizons [3].

2.1. Persistence Model

It is used as a model to test the prediction accuracy of a proposed model and is also considered a criterion for other models [32]. Simply put, this model only requires historical data from previous studies [33]. These methodologies are considered unsuitable for long-term forecasting and give better results for forecasting the very short and short-term for some time from some seconds to 6 hours [34] and it is more widely used for one hour for forecasting solar energy production [35]. Simply put, the solar data values should be similar to the energy values measured on the next day [36]. The solar energy output is expressed by the following equation [37].

$$Pf\ t\ +\ h\ =\ Ppd\ (t) \tag{2.1}$$

where $Pf\ t\ +\ h$ is the expected power output and $Ppd\ (t)$ is the power output from the previous day to the expected day in the same period. In many studies, the use of persistence model allows for better results compared to other methods. In Ahmad's study, where he explained the percentage difference between the persistence methods and the methods of machine learning is less than 2.5% [38]. In the study of Sanfilippo eat al. as well as a study by Martín et al. it showed a percentage of less than 5% in a comparative study they conducted between the method of machine learning and the

methods of stability [39], [40]. In a study by Lauret eat al. for the solar forecast an hour ago, it was shown that the accuracy of the prediction depends on clarity and clear sky conditions, and the percentage difference reached 2%, and the non-linear methods improve the gradual stability very little [41].

And the results of a difference appeared for the unstable sky conditions, the difference is clear between the machine learning and the fixed models, with an average of Nrmse to 2%. persistence models are sometimes as effective as complex models [43], [44]. And sometimes it excels and is better than svm [40]. In conclusion, as mentioned earlier, persistence models can be interesting, but it must be taken into account that the dynamics of the atmosphere have a direct and strong impact on forecasting, especially if the time horizon is more than one hour, so this model is intended for very short time horizons.

2.2. Physical Models

Physical models are a collection of mathematical equations that explain the physical condition of the atmosphere as well as its dynamical movements [42]. These physical models are made utilizing the characteristics of solar power plants. and wind turbines as well as geographical locations. These models are based on numerical weather predictions (NWPs) based on weather variables such as temperature, wind speed, intensity, pressure, etc., geographical location and historical trend data. It is basic when solar is only used, but after adding additional parameters, it becomes complex [43], [44]. When atmospheric variables are stable, prediction accuracy becomes better [45]. Physical models are considered reliable when predicting the medium and long terms but inaccurate in the short term [46]. According to various studies carried out by Dolara et al. and Gandelli et al., the physical prediction model has been combined with machine learning models as a form of a hybrid model to improve prediction. Despite this, the forecast accuracy was sensitive to weather conditions, so these models were suggested that to be applied in special sites or factories to improve forecast accuracy [43], [47]. Therefore, these models did not attract the attention of researchers, and they turned to other modern methodologies that are better and outperform the physical models in performance [44].

Simply put, statistical models represent a linear relationship between the historical time-series data as well as the intended result [48].

The relationship between the data and the mathematical equation is described as a clear linear relationship [31]. They can be easily formulated and used for short-term predictions, however in studies of the literature few predictions are used in this way [49]. using the equation below can be used to represent the ARMA model, which is a mixture of the commonly used and well-known moving average (MA) and autoregressive (AR) statistical models. [50].

$$x(t) = \sum_{i=1}^{p} \alpha_i x\,(t-i) + \sum_{j=1}^{q} \beta_j e(t-j) \qquad (2.2)$$

where *x(t)* represents the forecasted PV power, which is the summation of the AR and MA functions. Hence, p and q indicate the order, αi and β_j *are the AR and MA models'* coefficients, respectively. e(t) is white noise, which generates random uncorrelated variables with constant variance and zero means.

The main reason for the importance of this model is its ability to distinguish statistical properties and take the box-Jenkins method [51]. There is also a model called the AR integrated part MA (ARIMA) has wide uses and has an acceptable level of accuracy in prediction, which is the mainstay of the ARMA model [52]. The ARIMA model removes non-stationarity data by integral shear [53]. In research, Pasari and Shah employed an ARIMA model to forecast temperature and wind speed, and they came to the conclusion that the model is universal and requires certain adjustments, such as expanding the amount of data input [54]. Atique et al. studied solar energy forecasting and used the ARMA mode. It was concluded that this model requires constant data, so they converted the seasonal non-fixed data to fixed [55]. An ARMA model in some other form considering external input is the auto - regressive movement averaged (ARMAX). This approach is not dependent on the sun's radiation but rather on meteorological conditions, unlike the ARIMA method. In the study of Li et al., use ARMAX model and input weather characteristics such as temperatures, pressure, wind speed and direction, brick, duration of insolation and amount of precipitation to predict

PV output one day in advance and based on performance parameters. The model outperforms ARIMA, Radial Basis Function Neural Network (RBFNN), and other approaches. RMSE (125.84 W/m2), MAPE (82.69%), and mean absolute deviation (MAD) were the performance metrics (98.61) [56]. They provide an acceptable short-term prediction accuracy of up to two days and yet fail to make a long-term and stable [49]. After these studies, the researchers started using other hybrid methods, a mixture of statistics and artificial intelligence methods, to solve the problems of future forecasting methods.

2.3. Regression Models

It is a statistical technique for establishing a connection between both the explanatory and the relationship between variables. When using PV energy, the predicted energy is the regression coefficient, while the atmospheric factors are the responsible factors. In research by Keshtegar et al., four different types of regression models were employed to evaluate their accuracy in Turkey: Kriging, Response Surface Method (RSM), Multivariate Adaptive Regression (MARS), and M5 Model Tree (M5 Tree) for modeling solar irradiation. They use a wide range of data, such as high and low temperatures, duration of sunshine, velocity of wind, and relative humidity. The solar radiation was estimated from two stations in Adana and Antakya, the station located in Adana gave better prediction accuracy results for mars type than kriging RSM m5, and the station located in Antakya type M5 showed better results than MARS RSM M5. The results were improved by entering periodic data, and the Kriging type showed the best results in Antakya and Adana [57]. In a comparative study, Abuella and Chowdhury used a multiline regression model to predict solar energy and, in another study, Lauret et al. employed three distinct probability models to forecast events occurring 1-6 hours beforehand. The author applied numerical weather prediction for the following day's radiation as an external input when applied in two distinct places, and historical data for radiation from the sun as an internal input. The PV power output was predicted applying both simple and complex linear regression techniques. The constraints of this model are that it requires a large number of inputs at once and that the findings reveal that the linear regression model performs better when two inputs are used than when one is [58], [59]. Wang et al. created a structured partly functional

linear regression model (PFLRM) to forecast the PV production one day in advance and showed better results and improved prediction accuracy compared to Multiple linear regression (MLR) and RBFNN according to the performance value of MAPE, where the value of PFLRM showed 11.34% and the value of MLR was 20.92 % and the value of RBFNN was 63.88% [60]. Although regression models give results with more accurate prediction in some applications, they cannot be relied upon and generalized because they depend heavily on input data and need explanatory variables to improve prediction accuracy [61].

2.4. Machine Learning

Artificial intelligence is the ability to think, create, recognize patterns, make decisions, and learn from experience. It emerged as a major in computer science and has produced several powerful tools of practical use in engineering fields to solve difficult problems that require human intelligence. Artificial intelligence techniques have a very important role in modelling, analyzing and forecasting renewable energy systems and can be used as a way to address complex and undefined problems. they can learn from examples and tolerate errors so they can deal with incomplete data, once trained and they can make predictions and generalizations quickly. According to the results published in the various papers, it is a testament to the ability of artificial intelligence to predict faster, more accurately and more practically than any other traditional method in renewable energy processes [62]. Therefore, in the past few years, a focus has been placed on artificial intelligence techniques, many models have been developed to predict and take them as an alternative to traditional models [63]. This duality consists of three main types, which are machine learning, artificial intelligence, and deep learning. Figure 2.2 shows the difference between these types and their applications [64]. In the following sections, we will present modern methods based on the ML methodology on solar energy.

ML is a training process that automatically predicts the outputs of certain systems and is trained with what is available using a set of inputs and outputs. It allows the computer, as opposed to models that rely on statistics, to learn from this data via experience. ML can adapt to unstable data and deal with non-linear systems. These are

what made them reliable methodologies in the accuracy of forecasting and their outputs, and it is generally used for any data processing and analysis studies [65]–[67]. This technology consists of three main types, and according to the survey, it is the most widely used type to predict solar energy output.

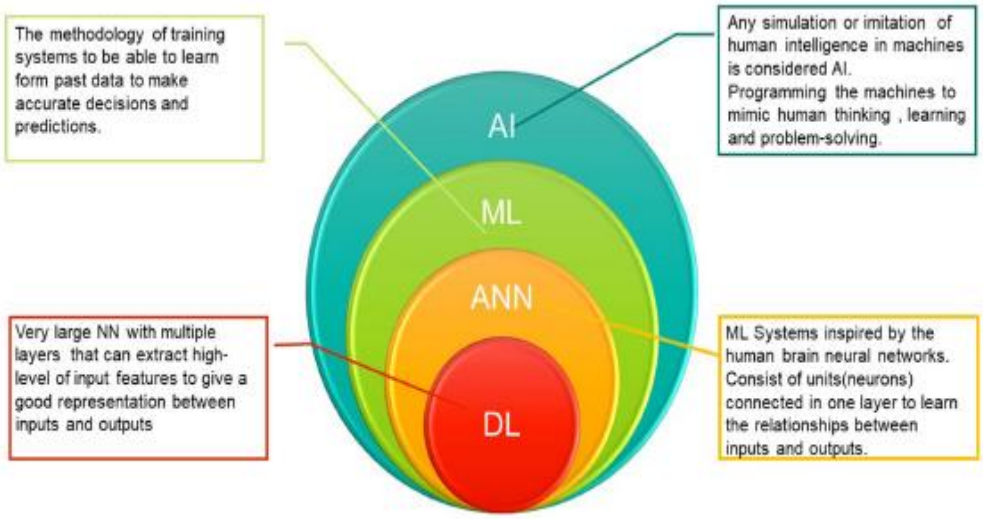

Figure 2.2. The relationship between types of artificial intelligence and their applications [64].

2.4.1. ANN

Ann is regarded as the most reliable method for forecasting renewable power output in response to shifts in weather conditions. However, when compared to statistical techniques, it is the most suited because of its limited skills for analyzing non-linear datasets. There are three main layers in all types of Ann: the input layer, which has an input feature so that each neuron can take one, the output layer, which determines the output's goal, and the hidden layer, which connects the input layer and output layer and is where all the necessary calculations are done. In order to assign any input to any output of any data and to provide activation functions for the ANN network that help to find any complex relationship between the input data and the output data, each layer in the neural network attempts to learn specific decimal weights that are determined at the conclusion of the learning process. This process is known as global approximation. The basic artificial neural retina of an artificial neuron and represents the equivalent model and can be expressed Curse with the following equation [32].

$$U_N = b + \sum_{j=1}^{N} (w_j \times I_j) \quad (2.1)$$

where U_N, w_j, I_j, b, N are the ultimate output of the network, connection weight, input quantity, bias weight, and other inputs, in that order.

In a study carried out by Karami et al., a model was used to develop Ann using ten groups for four variables of weather to estimate the output of PV energy. They applied it for a week over 4 seasons. The outcomes demonstrate that the ANN model, which uses 27 cells in the hidden layer and 4 neurons in the input layer, produces results that are quite satisfying. A deciding factor of 0.9972, 0.9856, 0.9487, and 0.9942 for summer, breach, winter, and spring, respectively, indicated that the accuracy of the forecast was dependent on the season [68]. Two ANN models were utilized in the work by Geetha et al. to forecast solar irradiance based on atmosphere balances. Training and testing data for the models were gathered from 6 distinct locations using the backpropagation technique [69]. In a study by Mohammad et al., they designed four multi-layer artificial neural networks (MLANN) structures with return to forecast PV Solar electricity production in Iraq from July 1 to August 31, 2018, between 7 am to 6 pm and they used the input data, temperature, radiation, output voltage, current and power. The model showed that MLANN had high accuracy and the model was affected by the number of hidden neurons to improve prediction accuracy [70]. Lopes and Hajimirza compared the performance analysis of 4 models of ANN to forecast PV Solar power output. They used localized PV data and online remote data for meteorology. The findings demonstrated significant accuracy in handling meteorological information that is adequate and helpful for planning PV installations. When it comes to PV data, it produced positive results for usage by power providers [71]. In their study Abuella and Chowdhury showed that the 14-entry Feedforward neural networks (FFNNs) methodology can give results that are superior to the multi-line regression methodology for solar energy forecasting. And they also showed that the data settings and their demonstration helped greatly to improve the training process's simplicity and effectiveness ANN. Additionally, their findings indicated that removing the nighttime hours from either the inputs somewhat improved performance. The prediction showed that the hours, when the sky was clear, give reliable predictions,

unlike the hours when the sky appears overcast with clouds and rain. This was one of the problems related to solar energy forecasting [72]. To solve this problem O'Leary and Kubby suggested input masking techniques which depend on groupings of error in a specific time scale. They recommended categorizing the hours into four groups: daytime, nighttime, sunrise, and sunset. The outcomes also demonstrated that masking inputs can enhance the approach's prediction output. They proposed using the same methods across various locations and circumstances to increase the ANN rating by approximately 1.3% and also to underline how crucial it is to hide these entries [73]. Ann was cross-hybrid with Articulated Neural Rendering (ANR) by Ozoegwu to increase the correlation factor for the monthly solar prediction by 9% and decrease the number of inputs ANR. And this provided a memory that helps to stabilize and generalize the prediction. Using data from multiple climates in Nigeria and the results of this methodology are good for the prediction of in the long run. Itis suitable for solar energy scheduling applications [74]. Bhaumik et al. used a multilayer feedforward neural network (MLFFNN) to predict solar radiation for 2016 by using hourly radiation data from 2011-2015. The data was sampled by taking 1 of photovoltaic geographical information system (PVGIS) 31325 data. Using time and day values as input parameters month, longitude, latitude, altitude, slope and high solar radiation were taken as outputs. The results showed a high accuracy of 98.74% and this showed the reliability and accuracy of the methodology used in this study [75]. To forecast global solar radiation for two distinct locations, Hashunao et al. suggested two multi-layer feed-forward back-propagation (MLFFBP) models. Data were gathered over a 5-year period to train the model, and the results demonstrated agreement with the actual output, allowing it to be used to the prediction of solar radiation by demonstrating that the MSE and R sections' performance values are almost zero and that the examined site's percentage is greater than 92% [76].

2.4.2. Recurrent Neural Networks (RNN)

It is a subtype of ANN and it is good at learning computational structures and complex relationships. It works powerfully when the data is important and affects the upcoming predictions. So it is considered one of the important and widely used tools for time-series predictions [77], [78]. As mentioned in our previous discussion, FFNN does a

good job of associating a set of inputs with outputs and learns independently without any memory of the previous outputs. Yona et al. mentioned that the errors are significantly reduced by using RNN compared to FFNN when they made a prediction 24 hours before the output of the PV power and the results appeared that the RNN was significantly superior to FFNN and also confirmed the validity of the results by simulation [77].

Geetha et al. proposed a short-term-based RNN algorithm to estimate PV power generation. It used data from sensors installed at the site where solar energy was installed. The experiment was for three periods: 5 to 15 minutes, 1 hour and 3 hours. The results showed that short-term memory based on RNN give the best results. for short-level prediction [79].

RNN is good for solving complex problems of time series prediction and stores the input data but fails to hold it for a long time. To address this issue, Hochreiter and Schmidhuber introduced the Long Short-Term Memory model for RNN (LSTM) [80]. The transmission of knowledge from earlier examples into long-term memory is regulated by this paradigm. The forgetting gate, the input gate, and the output gate are some of the gates that it has and consists of. This gate serves to determine if this information is kept or forgotten, and thus the model builds a long-term memory. Thus the model solves the problems related to the RNN which is fading [81].

Sabri and El Hassouni used real data from 1BDKASC Springs in Australia to perform a comparison study between the RNN and LSTM models to forecast the production of PV electricity. MAE, MSE, R^2, and root-mean-square error (RMSE) comparison between the two models revealed that the LSTM model surpasses the RNN in performance and can forecast stability as well as increase accuracy [82].

A comparative study was carried out by Ananthu and Neelashetty to show that LSTM networks are more accurate in predicting time series. They analyzed a large number of time-series data to predict solar power generation. Sampling data for two years previously recorded for power generation of 100 kW for 720 days was tested on 220 samples per hour to estimate monthly and daily solar energy generation and compare

the results with other models such as ARIMA SARIMA RNN fbProphet based on RMSE-based results show that LSTM gives better results than other models [83].

We look at the success and accuracy of LSTM in prediction compared to the models we referred to in previous studies, but they suffer from the problem of a large computational burden that may cause a slowdown in the LSTM network.

Cho et al. designed the Gates Repeated Unit (GRU) to solve this problem [84]. Its function is to combine a unit between the ratio gate and the input gate of the LSTM network. It contains only two gates, the first is reset and the second is refresh. Thus makes GRU faster than LSTM, but also it is not qualified for some problems. Because it has less computing power compared to LSTM [85].

This work by Hosseini et al. used GRU and LSTM to evaluate the univariate technique and the multivariate approach and estimate the hourly direct sun radiation. They found that GRU performed much better than LSTM from a computational standpoint. Because LSTM takes more time with no significant superiority[86].

However, GRU fails computationally in its ability to treat long-term consequences as demonstrated by Jebli et al. In a comparative study of the prediction accuracy of three models of RNN LSTM GRU for real-time solar energy forecasting based on meteorological data for the Errachidia region in Morocco from 2016 to 2018, 6 measures of efficiency performance were established, including mean absolute error (MAE), mean squared error (MSE), RMSE, mean error (ME), and R^2, or normalized root mean square error (NRMSE). By contrasting RNN with LSTM's propensity for dealing with long-term effects, the results demonstrated the superiority of RNN over LSTM. They also showed very high accuracy and fewer errors compared to RGU [87].

2.4.3. SVM

When training an ANN, a local minimum problem might occur. The support vector, a supervised machine learning technology, overcomes this problem. SVM is based on the kernel learning technique [88]. SVM offers a fundamental idea for mapping

linearity as a future space and non-linear data in spaces. Support vector regression, which is based on the idea of statistical education and structural risk reduction, is another approach that has been created to address challenges with linear regression [89]. The key characteristic of SVM is the kernel function, which allows a collection of data to be mapped and shown in higher dimensional spaces. As a result, the mapping of that data in SVM can effectively anticipate non-uniform estimates like solar and wind energy and capture non-linear data [88]. It's described as

$$K = exp\left(-\frac{1}{\sigma^2}\left\|x - x_i^2\right\|\right) \tag{2.2}$$

where x and xi are the input and output vectors, respectively. Greater objectives resemble lower-dimensional input objects. [90].

Jang et al. developed a one-day prediction model for SVM (15-300 minutes) and the prediction results showed that the prediction accuracy of SVM is better compared to nonlinear autoregressive (NAR) and ANN, and it was noted that the prediction accuracy decreases with the increase in the time horizon [91]. In general, SVM is highly efficient in high-dimensional scans and relative memory efficiency. It also solves optimization problems in L training, so its performance is poor in large training data and the calculations are somewhat complex and expensive. To solve this problem, a type of SVM least-squares SVM (LSSVM) was used whose function is to convert inequality into equality constraints, reduce computational complexity and speed up training for ripple SVM [92]. A proper kernel function has a significant impact on the performance of both the SVM and LSSVM models. Linear kernel function, radial basis kernel function, polynomial kernel function and wave kernel are the most common and used functions in SVM assembly.

In general, the SVM model can outperform other ML techniques and it can also tolerate noise and data changes positively [93]. The superiority of the SVM technology has been demonstrated by Quej et al. When they compared SVM with adaptive network-based fuzzy inference system (ANFIS) and ANN to estimate global solar radiation in highly humid regions. Solar irradiance in highly humid locations is very chaotic and affected by cloud coverage and precipitation. So that the solar radiation in

the locations where the humid areas are highly chaotic and affected by cloud cover and rain. So that rainfall was included as an input for the three ML techniques that were mentioned. The outcomes clearly demonstrated SVM's superiority; both other approaches were comparable and of little significance [94]. Ahmad et al. proposed four different SVM models to predict the generation of PV energy depending on the seasons. The four models were trained individually. As the inputs of the SVM historical data on weather and PV information were used. They adopted the RBF kernel and the polynomial kernel to determine the appropriate function for each of the four models. The results showed that the RBF kernel performs. The performance is better to predict the accuracy of the PV module, on the other hand, the polynomial kernel shows a decrease in MSE and MAE to predict the production of PV energy based on the prediction accuracy[95]. In a study carried out by Hamamy and Omar to predict solar radiation at different time horizons, they applied the LSSVM model with the RBF kernel and to build the model, they entered the sunrise periods and weather data as input of the model and concluded that the LSSVM model shows better accuracy results for prediction for a short period and the accuracy decreases for long periods [96]. These are consistent with the results and conclusions obtained by Liu et al. The LSSVM model was not a model with appropriate accuracy for 48 hours before prediction. Malvoni and Hatziargyriou addressed the weakness of LSSVM for long-term prediction by hybridizing it with a 3-D waveform for 24-hour prediction[97].

2.4.4. Levenberg–Marquardt Algorithm (LMA)

The ELM model was first proposed by Guang-Bin and Qin-Yu [98]. And the goal was to train single-hidden layer feedforward networks (SLFN) which were different from gradient-heaping methods that allocate random values between input layers, hidden layers and biases in the hidden layer. It is fairly similar to previous methods, with the exception that it just learns the weight in between the hidden and the output layers layer and it does not repeat learning any other parameters [99]. It is widely used in learning problem applications such as classification, regression, clustering and feature mapping, and then developed with numerous suggestions to further improve stability for specific applications[100]–[103]. The loss function in the ELM model depends on second-order statistics. It cannot apply and fails to perform with non-linear and non-

Gaussian data. When used, it is combined with optimization algorithms or other techniques to augment. In a study by Tang et al., the entropy method and ELM method were combined for a period of one or two hours. The findings revealed that MAPE resulted in a decrease of 2.5538% in CPU time (measured in milliseconds) and an increase in values for R^2 (0.99292). They claimed that the technique's good predictive accuracy, fast convergence, and minimal parameter adjustment made it ideal for forecasting PV output. When compared with GRNN and RBFNN, however, minor differences were shown by the value of R^2 compared to RBFNN [104]. A comparative study was conducted to train two RBF and ANN nuclei using the Levenberg–Marquardt algorithm and the ELM to predict PV power in hours and days for three different networks. Over long periods, its capacity was high compared to other models, and they also made it clear that it was not possible to include external data and suggested the treatment in future work [105].

2.5. Hybrid Methods

Hybrid methods are the methods combined from two or more models with some optimization algorithms. This method increases the prediction accuracy of the general hybrid system by combining some of the individual features of each model. Through previous studies, it became clear that in most cases are not enough one method or one model to obtain an accurate and reliable prediction of PV energy. Therefore, modern methods are used to improve the accuracy of prediction by integrating two or more models compared to using one model [43]. It will increase the computational complexity and the cost, space, structural maintenance, durability and reliability must be taken into consideration. The performance of each model individually determines how well the hybrid technique works. Poor performance will result in a weak model. If the performance is good, the results will be good [32]. The hybrid method also can improve the performance of complex systems through solutions to individual problems. With a group of the best appropriate techniques it is used in many applications of PV energy prediction Metaheuristic is a term used when proposing solutions to a large group of problems to improve, and it is one of the high-level research methods. In modern applications, many metaheuristics algorithms are applied in a successful and accurate form for problems that are difficult to improve. One of the

reasons that attract the use of these algorithms to solve complex and large problems is that they get solutions for them. Even if the size of the problems is very large, they are implemented in short periods compared to the size of the big problems.

Optimization problems that attract the attention of using metaheuristics algorithms have a large variance that is divided into several goals; restricted to unrestricted, continuous to non-continuous, and multi-objective. Implementation is impractical due to computational requirements when it is large data But the metaheuristics methodology provides an elegant and practical solution to many of these problems and is designed to arrive at the most approximate and ideal solutions to optimization problems [106]. To build accurate, efficient and inexpensive ML models to predict accurately and reliably, scientists have used metaheuristic optimization techniques with ML for different purposes to adjust the model, estimate parameters, train channels, and adjust hyperparameters related to the network structure[107].

The performance of ML models is improved by adjusting and optimizing model parameters such as Biases, weights, and/or penalties of kennel functions all are examples of ML model parameters. Therefore, a lot of descriptive features have been incorporated to improve the parameters of the ML approach.

2.5.1. Metaheuristic and ANNs

Cho et al. proposed a model for estimating the PV energy per hour by ANN and the optimization algorithm PSO. They used real measured data related to seasons and geographic regions. The PSO algorithm helped to improve the training processes of the ANN network to reach accurate and optimal solutions. The accuracy and reliability of the estimation was confirmed by the actual details of the PV power plant in different and measured areas. It helped greatly to meet the demand for load more accurately while coordinating with other traditional stations [108]. Bao et al. proposed a GA-NN model for predicting solar radiation and historical data include variables like ambient temperature, atmospheric pressure, as well as wind velocity [109]. Pedro and Coimbra tested the GA-ANN model for prediction of solar energy output for one and two hours without external inputs and compared it to other models such as ARIMA, K- Nearest

Neighbor (KNN) and ANN the GA-ANN model outperformed other models in the short term and likewise did not succeed in the long-term prediction, he said. [110], [111].

2.5.2. Metaheuristic and SVMs

We mentioned that tuning kernel parameters for SVM are one of the defects in using this method. Studies have been put forward to solve this defect with a combination of metaheuristic optimization algorithms. For example ,Wang et al. proposed a model to predict electric power generation based on PV in micro-networks using ABC-SVM to train weather data and PV power outputs and classify them as into 4 categories. They used PSO-RF (Random Forest) to train thousands of data for each set of classified data and that is how 4 individual trained models were obtained. To predict after obtaining the optimal parameters the model was improved by differentiating and training the data and obtaining the appropriate model. By using this method, they obtained a high prediction accuracy under different weather conditions [112]. VanDeventer et al. used the GA-SVM model method to predict the energy of a short-term PV system an hour earlier at Deakin University. The SVM model was used to classify historical weather data and then improved by GA. Through their analysis, the accuracy of the individual classifiers was greatly enhanced by the GA algorithm that was. The main step in increasing the accuracy was the difference in the superiority of the GA-SVM system over the traditional SVM system with a value of 669.624 Watts for RMSE and an error rate of 98.7648% for MAPE [113]. Niu et al. in their research, experimented with the (Ant Colony Optimization) ACO-SVM model to predict the power load in the short term. The proposed model obtained a higher prediction accuracy compared to SVM and Back Propagation Neural Network (BPNN). In this way, they were able to overcome the defects in large data and fast processing [114].

2.5.3. Metaheuristic and ELM

We mentioned earlier in the Single ELM Methodology section that when the ELM approach is based on an improvement approach, it results in reliable models and better performance. For example, in this study Behera et al. developed an approach for PV

power prediction based on ELM optimized with the PSO algorithm to increase the prediction accuracy and the results. The experiment was compared with BPNN, so the ELM algorithm showed better results. After that, they applied the PSO optimization algorithm for the PSO-ELM, accelerate PSO (APSO) APSO-ELM, and craziness PSO (CRPSO) CRPSO-ELM models. And the models were able to improve the ELM results. Therefore, the PSO optimization algorithm was able to obtain a generalized weight and bias which enabled ELM to achieve better results with a low error rate [115].

Mansoury et al. proposed an integrated model from ELM and the PSO optimization algorithm to predict the generated solar energy. The aim of which is to control the amount of energy generated to ensure the availability of energy supply by sensing the average energy per hour based on the previous hour's data using the variables of temperature, radiation and wind speed the results obtained were much better than those methods mentioned in the literature in terms of prediction accuracy and time convergence [116].

2.6. Summary

Machine learning model techniques (ANN, RNN, SVM, ELM) have been successfully used to predict solar energy according to many references and statistical evaluations with scales such as MAE, MSE, RMSE and R^2. They have been tested and confirmed their ability to predict and outperform various traditional methods.

In particular over the medium and short term, the non-linearity and chaotic characteristics of solar energy data were advantageously captured by the straightforward ANN architectures [110].

Nonlinear solar energy patterns can be mapped using a powerful ANN called (BPFFANN), although it is vulnerable to fluctuations and can easily enter local minimums. [117]. RBFANN model is used for predicting the problems of solar and wind energy, due to the speed of learning and less computational complexity compared to the usual BPFFANN [118].

There are many different types of ANNs. If the parameters are related to the training or the hill of the network, it directly affects its reliability [119]. To adjust these parameters, integration of different optimization algorithms is required and in some cases, it is time-consuming and large historical data is needed to train networks. RNNs are a special type of ANN that can preserve and use the advantages of previous time steps. This makes them able to learn and reach a temporal relationship between the data [120].

RNNs can form accurate prediction models, but they have a short memory problem associated with them and this causes training problems. GRU and LSTM are nodes introduced to solve the RNN regression problem. These nodes process data in various mathematical activation functions to take advantage of the time-step characteristics that preceded long memory periods. And their superiority is confirmed by activating time-series prediction with rather short training intervals. However, the use of this mechanism in different types of RNNs causes an accumulation of errors and leads to an explosion of scaling fears, which in turn affects the network training process [121].

The SVM model of ML is also powerful, well known for its global approximation ability and can simplify complex mathematical computations. Unlike an ANN that can learn small patterns of sorts from data sets with little dependence on prior knowledge [122]. However, performance is highly dependent on kernel function parameters and this requires the integration of optimization algorithms for tuning and training [123]. When the training data sets are large-scale, this leads to the instability of the prediction in the horizons of the long prediction [124]. One of the problems associated with SVM training is overfitting, and this requires taking different decisions during the training process [61]. One of the system improvement tools for estimating weights and appropriate biases is ELM [97]. Despite training and rapid convergence when training, the problem may appear that convergence is premature in some cases, and the model fails to predict accuracy and generalization. This is what encouraged thinking that integrates DL with ELM [63].

Integrating ML hybrid with metaheuristic are reliable and recommended solutions for forecasting accuracy. metaheuristic is developed to adjust the parameters of the ML

model or the network architecture. It aims to integrate the properties that achieve the necessary convergence, and this leads to high reliability and prediction accuracy compared to independent ML approaches.

Based on the investigation and review of previous literature evaluating the MSE, MAPE, R/R^2 SAMPE, RMSE metrics. The ML hybrid Model with descriptive characteristics is the model with the highest accuracy for prediction. A favorable population-based metaheuristic model integrated with the ML model is known for its ability to identify optimal global variables for different functions. Swarm-based evolutionary optimization techniques are a branch of population-based optimizers that are preferred by scientists for parameter optimization with ML modelling. Hybrid models can strongly determine the optimal values that exceed the independent improved values. Although hybrid models have given accuracy and reliability in prediction, they take more time to implement and require powerful computational machines in some cases, unlike individual models. Some researchers rely on experience and computational knowledge to adjust these parameters are super.

Finally, based on research in the prior literature, which includes a thorough analysis of the significance of enhancing ML-based prediction approaches in general and neural networks in particular, through 2022, this has been a significant and hot issue. The studies shown that the neural network could be improved by adjusting and adjusting parameters including weight and starting weight, overall rate and bias, number of hidden layers, number of nodes in the hidden layer, and activation functions. The reference research also concentrated on ANN-based metaheuristic optimization methods, including ANN-GA and ANN-PSO, and compared them in terms of training effectiveness, training duration, and needed micro-network administration.

From this review, its study of the previous literature emphasizes the importance of hybridizing the neural network by means of the metaheuristic optimization algorithm to search for the best parameters of the ANN to achieve the best structural network based on test results to improve the performance of the ANN by means of metaheuristic optimization techniques. While studying these reviews of the ANN-based optimization method.

- When data is big working with ANN is the best choose.
- Hybridization of ANN with metaheuristic optimization algorithms improves the results. But may slow down the training in some cases. It depends on finding the appropriate optimization method and the optimal values for the system.
- Conventional NN techniques create complex, sensitive and non-linear computation problems to obtain high accuracy and reliability, the appropriate optimization must be chosen for the system.
- By cutting down on time or utilizing ANN to identify the best data by minimizing trial and error and random selection, optimization techniques enhance neural network architecture.

SECTION 3

HARDWARE AND DATA ACQUISITION SYSTEM

In this section, information on how to produce power from a photovoltaic panel, hardware setup and how to quote the reference are provided.

3.1. Power Cell Working

A solar cell (also known as a photovoltaic cell or PV cell) is defined as an electrical device that converts light energy into electrical energy through the photovoltaic effect. A solar cell is basically a p-n junction diode. Solar cells are a form of photoelectric cell, defined as a device whose electrical characteristics vary when exposed to light, light can be produced from many sources, but the most effective light is sun light. Individual solar cells can be combined in series or in parallel to form modules commonly known as solar panels. The common single junction silicon solar cell can produce a maximum open-circuit voltage of approximately 0.5 to 0.6 Volts. When sun light touches the p-n junction, the light photons will enter in the junction easily, through very thin p-type layer. The light energy, in the form of photons, supplies sufficient energy to the junction to create a number of electron-hole pairs. The incident light breaks the thermal equilibrium condition of the junction. The free electrons in the depletion region can quickly come to the n-type side of the junction. Similarly, the holes in the depletion can quickly come to the p-type side of the junction. Once, the newly created free electrons come to the n-type side, cannot further cross the junction because of barrier potential of the junction. Similarly, the newly created holes once come to the p-type side cannot further cross the junction became of same barrier potential of the junction. Since the density of electrons is greater just on the n-type side of the partition and the density of gaps is larger just on the p-type side, the p-n joint will function like such a tiny battery. The term "photonic voltage" describes the induced electrical potential.

A current via the joint will be negligible if only a minor load is connected across it. Figure 3.1 displays the relationship between illumination and voltage output.

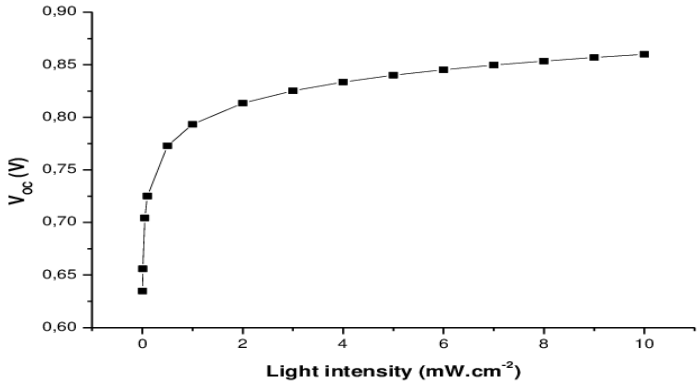

Figure 0.1. Solar cell output vs light intensity [125]

These applications necessitate the utilization of metals with band gaps closer to 1.5 eV. Silicone, Gallium arsenide, Cadmium telluride, and copper indium selenide are all frequently employed materials**.** There are some conditions of materials to be used in solar cell:

- It must have a band gap from 1ev to 1.8 ev.
- It must have high optical absorption.
- It must have high electrical conductivity.
- The raw material must be available in abundance and the cost of the material must be low.

3.1.1. Advantages of solar cell

1. No pollution associated with it.
2. It must last for a long time.
3. No maintenance cost.

3.1.2. Disadvantages of solar cell

1. It has high cost of installation.
2. It has low efficiency.
3. During cloudy day, the energy cannot be produced and also at night we will not get solar energy.

The Table 3.1. below are the data for the poly type solar panel used in our study.

Table 3.1. Table of electrical ratings for PV panel.

Peak Power (Pmax)	80	W
Voltage (Vmp)	16.6	V
Current (Imp)	4.55	A
Open Circuit voltage (Voc)	21.8	V
Short Circuit Current (ISC)	5.23	A
Maximum Bypass Diode		A
Maximum Series Fuse		A

3.2. System Set-up of The PV and Location

The PV panel and DAS that contains the sensor collection has been installed on the roof of the building of the Technology Department of the faculty of engineering, Karabuk university in the city of Karabuk, Turkey, which is located in a geographical location shown in Figure 3.2 at the coordinates of latitude 41.205, longitude 32.628 and height of 1.037. The sun is 15 hours and 9 minutes where the highest average low temperature around 16 °C, as well as the average high temperature, ranges from 29 °C. the humidity is 20% during the summer season in 2022. The amount of average shortwave solar energy generated decreased by 0.6k Wh from 6.9 kWh to 6.2 kWh.

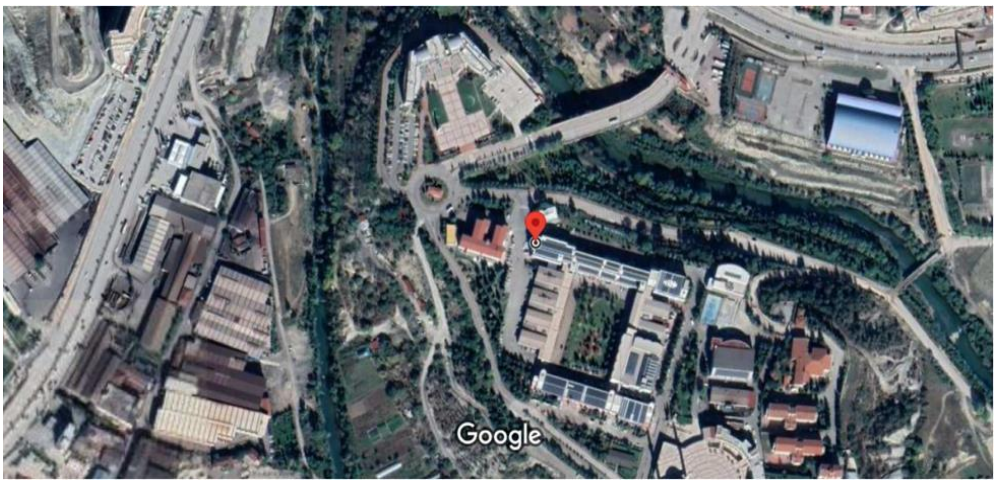

Figure 3.2. Location setup the photovoltaic panel and data acquisition device system (DAS).

The experimental data acquisition system consists of two subsystems, the first as seen in Figure 3.3.

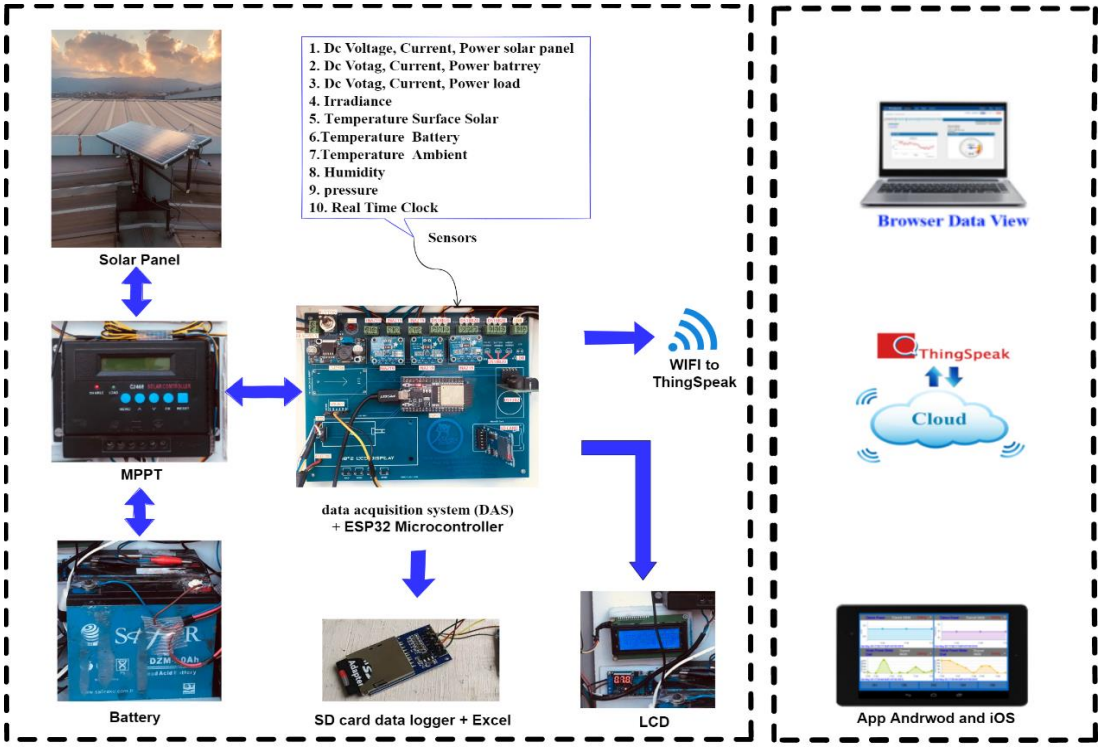

Figure 3.3. PV system setup block diagram: rooftop subsystem on the left and lab subsystem on the right.

One of them is on the rooftop which contains the sensors for obtaining data and archiving the site via SD card data logger and saving the data on an excel file. The other branch, which is located in the lab, is utilized for Internet-based data archiving and monitoring.

The rooftop system consists of PV panel modules are installed at an angle of 18°, data acquisition circuits for all weather and electrical parameter sensors, an esp32 microcontroller containing Wi-Fi, a dc-dc converter and a solar controller MPPT for the modification of pulse width (PWM) signal output. A real load consists of three fans and is used to cool the contents of the DAS.

The subsystem in the laboratory records the data from the subsystem in the rooftop and is monitored and recorded at specific time intervals through an open-source IoT

platform called Thingspeak and communication between the two systems is via the esp32 microcontroller that contains the internal Wi-Fi.

3.3. Measurements

In this study, a DAS with 6 environmental parameters and 9 electrical parameters is developed. The DAS was designed internally for flexibility and to make signal adaptation circuits for some sensors that fit the parameter values we need.

Figure 3.4 shows the sensors and adaptive circuits that were chosen in order to create a reliable and weatherproof DAS on location.

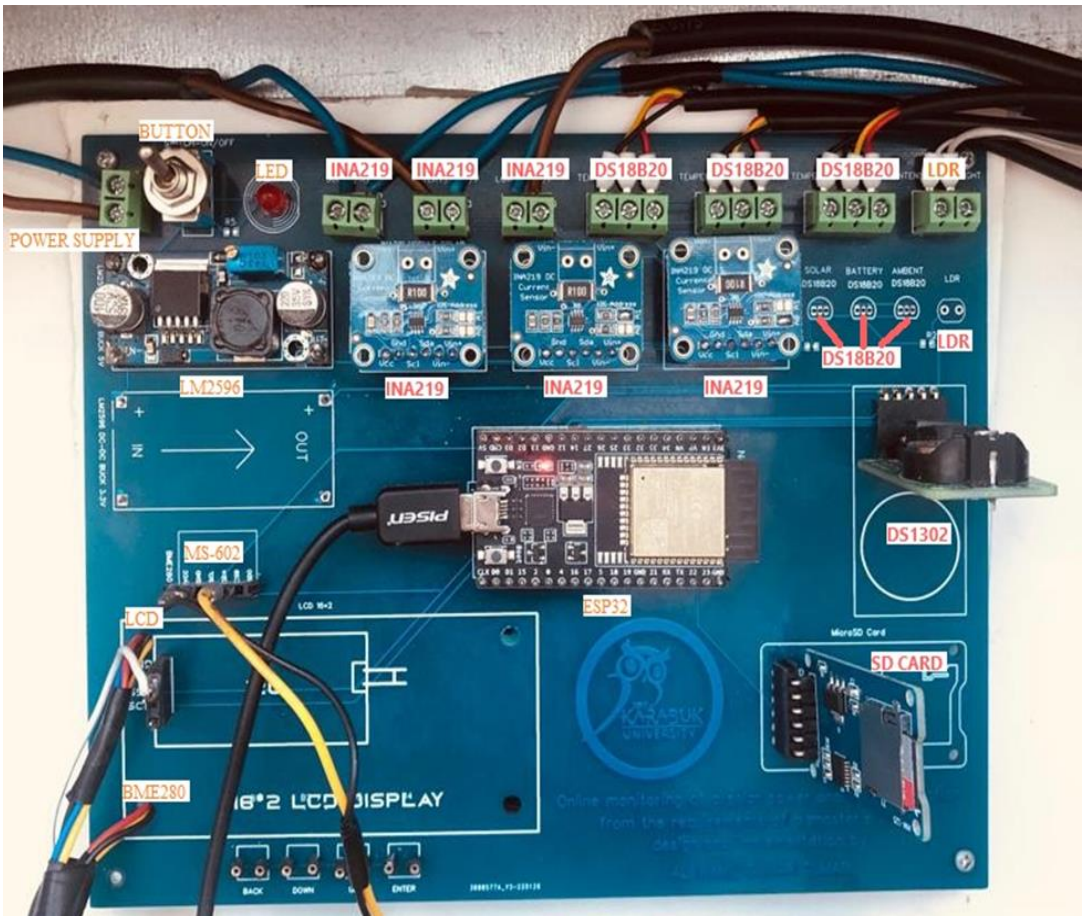

Figure 3.4. Data Acquisition System (DAS).

The measurements and sensors are included in Table 3 together with the production source and measurement parameter.

Table 3.2. Table of specifications of each sensor.

Parameter to be measured	sensor	Manufacturer/Model	Measurement range
Dc Voltage, Current, Power for the solar panel, battery load	INA219 High Side DC Current Sensor Breakout	Texas Instruments,	2W current sense resistor, 0.1 ohm Up to +26V target voltage Current measurement with a precision of 0.8mA and a maximum of 3.2A
Irradiance	MS-602 Pyranometer	EKO	0 - 2000 W/m²
Surface Solar, battery, Ambient temperature	DS18B20 Programmable Resolution 1-Wire Digital Thermometer	Maxim Integrated	-55 to 125°C
Humidity, pressure	BME280	Bosch	0 to 100 % 300 to 1100 hPa

3.3.1. DC electrical voltage, current and power

3.3.1.1. Sensor

The Ina219 is a bi-directional zero-drift bus voltage monitor module provided by Texas Instruments Inc. It features a built-in interface that can transport data to microcontrollers through SMBus or I2C. It has a versatile, programmable, high resolution 12-bit chip with 16 addresses and a double register that converts power to watts. Although the INA219 chip works on 3 or 5 volts, it is able to measure current and voltage with an independent external system and it can deal with measuring high side current up to +26 VDC. It also reports this high side voltage. Just connect the measurement input directly to a voltage source from 0 to 26 V which is very good for tracking solar panels and batteries. Since it can measure current and voltage, it can measure the power used as an I2C device that senses the switching is connected to the bypass voltage via an external resistance and uses the negative analog input to measure the load and with the measurement of current the power is dissipated in the load.

The chip contains an internal amplifier which means that you do not need to convert the level or amplify the voltage. The voltage is measured via the amplifier. The accuracy through the resistor is 0.1 ohms 1%. It can be measured up to ± 3.2 A because the input difference for the maximum amplifier is ± 320 mV. Accuracy at range ±3.2A is 0.8 mA with 12-bit internal ADC, maximum current is ±400 mA, accuracy is 0.1 mA with the internal gain set to minimum.

3.3.1.2. Calibration

A multimeter was used for calibration in order to compare the measurement findings between both the calibrator as well as the sensor, optimize performance, improve reading accuracy, and check the linearity of the signal. They significantly affect how well the measurement system performs. The objective of these tests is to know the accuracy and readings of voltage and current between the sensor and the calibrator. The INA219 sensor is calibrated in the laboratory with an accuracy of ± 0.10%.

3.3.1.3. Wiring

The sensor is connected via I2C protocol, so we need to change the I2C address. We use 3 each for the solar panel, battery, and load. Figure 3.5 showed the three locations of the sensors.

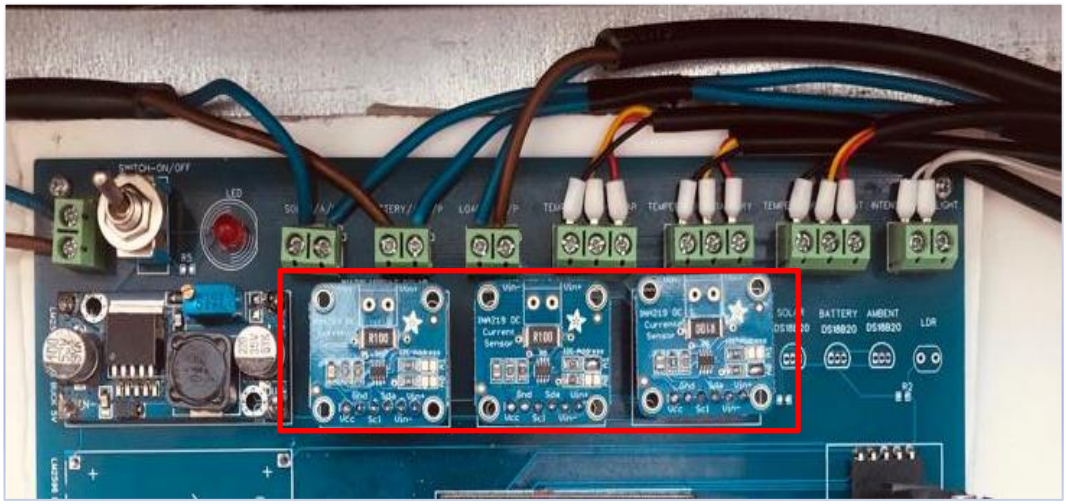

Figure 3.5. INA219 voltage, current and power sensor.

It has two inputs A1 and A0 which are two lower bits that are multiplied in the same way as ADS1115. That means the inputs can be set to GND, VCC, SCL and SDA. The addresses of the sensor board A1 and A0 are pulled to a low level by the resistors so that when soldering two points it is allowed to give a different band address and the addresses can be changed. Sensor and circuit wiring: We connect V+ to the circuit's power supply's positive terminal. Connect V- to the load's positive terminal. Then the sense resistor is connected. Connect the power supply's negative terminal to GND. The sensor can monitor load voltage and current with this connecting method.

3.3.2. Irradiance

3.3.2.1. Sensor

The MS-602 pyranometer sensor is a part of the EKO pyranometer series for measuring solar radiation based on heat. It is considered one of the most economical measurement solutions in the EKO company industry. The sensitivity and affordable cost of such a sensor are two of its best features. It is integrated into all weather conditions and is found in many meteorological balances and small professional photovoltaic sites.

The sensor contains an internal and external glass dome. This sealed dome provides an environment for the detector and protection from influencing factors such as dirt, rain and wind. In addition to the mechanical aspect and the optical properties of the glass dome reduce the unwanted effects from the Earth's atmosphere as it prevents infrared contrast. Glass domes allow global solar radiation measurement of all EKO thermostats with a 180-degree field of view. Figure 3.6 shows the installation angle of the sensor.

When sunlight hits the black side of the detection, the sensor produces a voltage that increases in relation to the amount of light absorbed. And, thanks to the high black absorbent material, very stable and timely measurement is ensured for most of the measurement features such as response time, non-linearity, sensitivity, zero offset B, etc.

Figure 3.6. MS-602 pyranometer sensor.

3.3.2.2. Calibration

The data acquisition system defines a measurement range in which the signal can be measured with an accuracy range from 0 to 10 mV. The global broadband solar radiation does not exceed 2000 $W\ /\ m^2$ in all horizontal and tilt measurement positions and the maximum level of the output signal voltage is 10 mV. Calculating the maximum output voltage requires multiplying the maximum solar radiation value by the calibration factor. For example, the sensitivity of the calibrated temperature scale is 0.005 $mV/W\,.m^{-2}$ and the maximum solar radiation is 2000 $W\ /\ m^2$, the maximum output voltage is 10 mV. We have created a signal amplification circuit to convert the voltage output from 0-10 mV to 0-5 V so that the controller can read it. The output voltage $E\ (mV)$ is divided by the sensitivity of the pyranometer S ($W \cdot m^{-2}$) and Equation may be used to compute the total solar irradiation.

$$I(W\ /\ m^2) = \frac{E(mV)}{\mathrm{S}\ (mV/W \cdot m^{-2})} \tag{3.1}$$

The sensitivity S is a fixed number on the product and can be calibrated by checking the sensitivity of the sensor.

3.3.2.3. Wiring

First, it must be ensured that the cable is not exposed to direct sunlight wind or rain by lining the cable through a cable channel.

These effects may cause a detractive signal. It is also isolated well to make sure that it is not affected by the weather conditions and by magnetic emissions. So, we must be sure to place it at a safe distance place from sources that are likely to emit electromagnetic noise such as high voltage lines and AC power sources.

We connect the output cable to the sensor directly, making sure that the other end of the output cable is connected to the continuous voltage signal amplification circuit that we designed to amplify and strengthen the output signal as in Figure 3.7. Because the sensor's output signal is very small and the controller cannot accurately record and read it. So, we amplify the signal and convert it from 0- 10 mV to 0-5 mV.

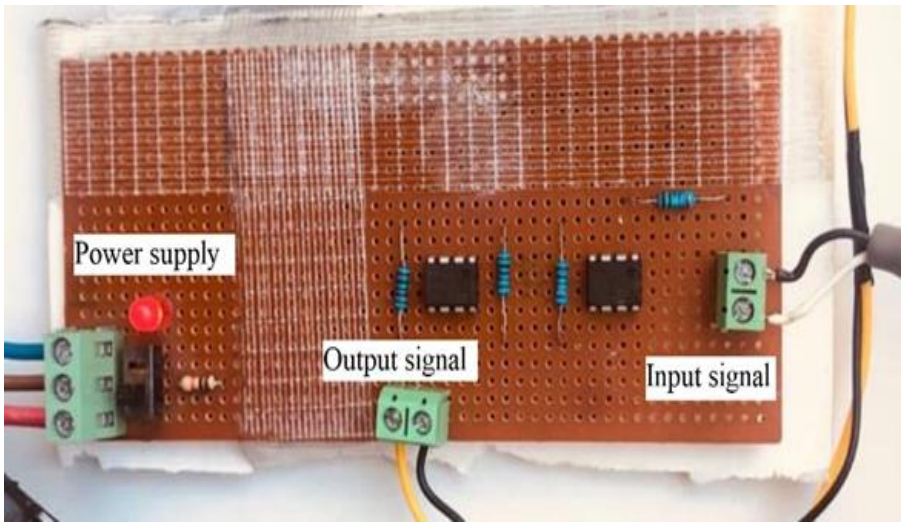

Figure 3.7. Signal amplification circuit.

We used uA74 type Op-Amp (operation amplifier) in the amplification as the electronic device. The circuit consists of two stages; the first one is to amplify the signal and the second one is to strengthen it with the use of a section of resistors as a sample to get the appropriate amplification from 0-5V and a symmetrical external supply source 12V.

3.3.3. Temperature

3.3.3.1. Sensor

The DS18B20 can measure the surface temperature, ambient temperature, and battery temperature of a solar panel, a single-wire digital temperature sensor by Dallas Semiconductor Corp. It requires a single data line to communicate with the controller. It can be powered by an external power source or draw power from a data line (called "parasitic mode"). You can find two distinct variations of the DS18B20 sensor module. One of them operates similarly to any other transistors. The other comes with a waterproof probing that may come in handy when taking readings from a great distance.

This method is fairly precise and can function with no additional parts. The ds18b20 sensor provides temperature readings from -55 degrees to +125 degrees, with an error of only 0.5 degrees. The sensor has a preset resolution of 12 bits (0.0625°C), but the user can change it to 9 or 10 bits to fine-tune the precision. Figure 3.8 showed the three locations of the temperature sensor.

Figure 3.8. DS18B20 temperature sensor.

In order to make it simple to identify between them, the sensor includes a 64-bit serial code that is closed at the factory. The benefit of this sensor being able to cohabit on the same 1-Wire bus is its finest feature. It is a big advantage when we want to control many ds18b20 sensors.

Employing this feature, that we used multiple sensors of the same type and distributed our scientific message to different places.

3.3.3.2. Calibration

The DS18B20 is an accurate temperature sensor between -10 and +85 degrees Celsius, with a sensitivity of 0.0625 degrees Celsius and an operating temperature range of -125 degrees Celsius up +125 degrees Celsius. The linear scale voltage of the temperature sensor is 10.0 mV/°C.

To calibrate a temperature sensor, we must measure something whose temperature we know or use a known reference. We used two methods here for calibration. The first one is the location of the weather conditions. The correct temperature values were confirmed by experimenting with the sensor on boiling water. As we know that boiling water boils at a temperature of 100 ° C. As for the second method, it is to monitor the temperature of the temperature from the sites specialized in the weather conditions to make sure that the temperature is within the required and reasonable range during the working period of the sensor.

3.3.3.3. Wiring

We connect three DS18B20 sensors to the microcontroller and display all values for the sensors in degrees. It only requires one pin of the microcontroller to connect multiple ds18b20 temperature sensors using the I2C protocol.

In order to measure anything far away or in rainy conditions, we employed a waterproof sensor. The cable is PVC-coated and since the sensor is digital, there is no signal deterioration. It is pretty accurate with an error rate of ± 0.5 ° C and can give

12-bit accuracy when converting from digital to analogue. We use a 1-wire protocol. We connect a resistance of 4.7 kΩ which is required as a pull from DATA to the VCC line.

3.4. Microcontroller and Dataset Archive

3.4.1. ESP32-WROOM-32

The ESP32 development board is an integrated Wi-Fi controller launched by Espressif Systems in China after the ESP8266 chip. It has stronger performance than the ESP8266 which has a dual core LX6 processor and can be used to develop more complex applications. Figure 3.9 shows the general structure of the microcontroller.

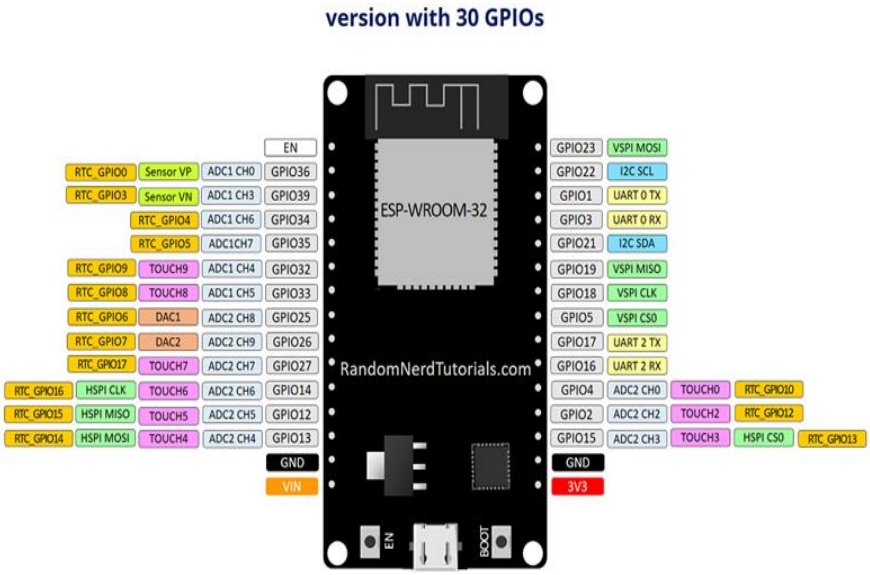

Figure 3.9. ESP32-WROOM-32.

The ESP32 chip or module has the following characteristics:

- Included in the package is a Tensilica LX6 a double processor, of which one core is designed to handle increased communications while the second core is used for developing standalone apps.
- 32-bit (dual core) processor main frequency and CPU normal operating speed 80 MHz up to 240 MHz.

- The 4 Megabytes of RAM, 448 Kilobytes of ROM, 520 Megabytes of SRAM, and 4 Megabytes of flash memory (for storing programs and data) are more than enough to process the massive string that makes it up modern internet content, Javascript object records, and all we frequently send on IoT.
- Support up to a maximum of 16 MB for devices using the Serial Peripheral Interface (SPI).
- The ESP32 integrates the HT40 Wireless Transceiver of 802.11b/g/n, so it can not only connect to Wi-Fi and interact with the Internet but also can set up its own network, permitting different devices to attach on to it.
- Supports WIFI Direct, a peer-to-peer connection method that works well without an access point. Compared to Bluetooth, WIFI Direct is simpler to set up and offers far faster data transmission rates.
- Operates at frequencies range of 2.4–2.5 Gigahertz.
- Bluetooth v4.2 is fully supported by that the protocols, which means that it can communicate at both the Bluetooth Low Energy (BLE) and the more traditional Bluetooth basic rate/enhanced data rate (BR/EDR) data rates.
- Supports a lot of peripheral interfaces such as general-purpose input/output (GPIO), ADC, Digital -to- Analog Converter (DAC), SPI, I^2C, Inter-IC Sound (I^2S), Universal Asynchronous Receiver-Transmitter (UART) and other common interfaces.

The ESP32's operational voltage spans from 2.2V to 3.6V; the 3.3V voltage on the board is reliably maintained via an LDO regulator. When the ESP32 draws up to 250mA during RF transmission, its maximum current output of 600mA should be more than sufficient. The board's MicroB USB port provides power to the ESP32 development board. Alternatively, the VIN pin may be utilized to directly power the ESP32 and its peripherals provided you have a 5V regulated voltage source.
The ESP32 chip may be programmed and communicated with using your computer thanks to a USB to UART Bridge controller from Silicon Labs that is included inside the CP2102 board.

ESP32 may be developed in a variety of methods, but the most popular option is to utilize the official Arduino kernel from Espressif for ESP32. The official Arduino

software support, easy to start, most of the programming syntax is compatible with Arduino and with the help of the Arduino environment, there are very rich resources that can be used directly.

3.4.2. Data logging and monitoring

Researchers and engineers always rely on data to design and improve a particular system.

Data recording and analysis is a common practice in most industries, and we recorded data in a certain period of time using an esp32 microcontroller to read the data and save it to the SD card, display it online on the computer, mobile monitoring using ThingSpeak and also displayed locally on the 20×4 LCD screen. Figure 3.10 shows data archiving and monitoring online and on site.

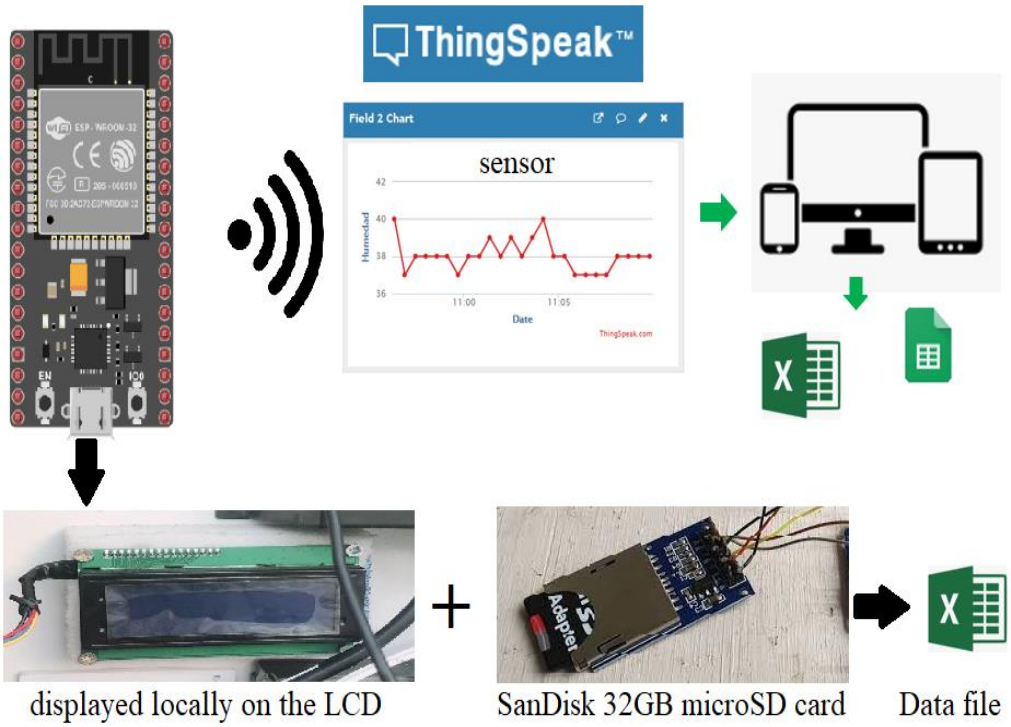

Figure 3.10. Dataset logging and monitoring by ThingSpeak, locally by Lcd.

Recorded data is saved to a text file stored on an original SanDisk Ultra 32GB microSD card. Time and date information is acquired using the ds3231 real-time clock board.

The following Figure 3.11 shows the data logger file (data.csv) generated by DAS.

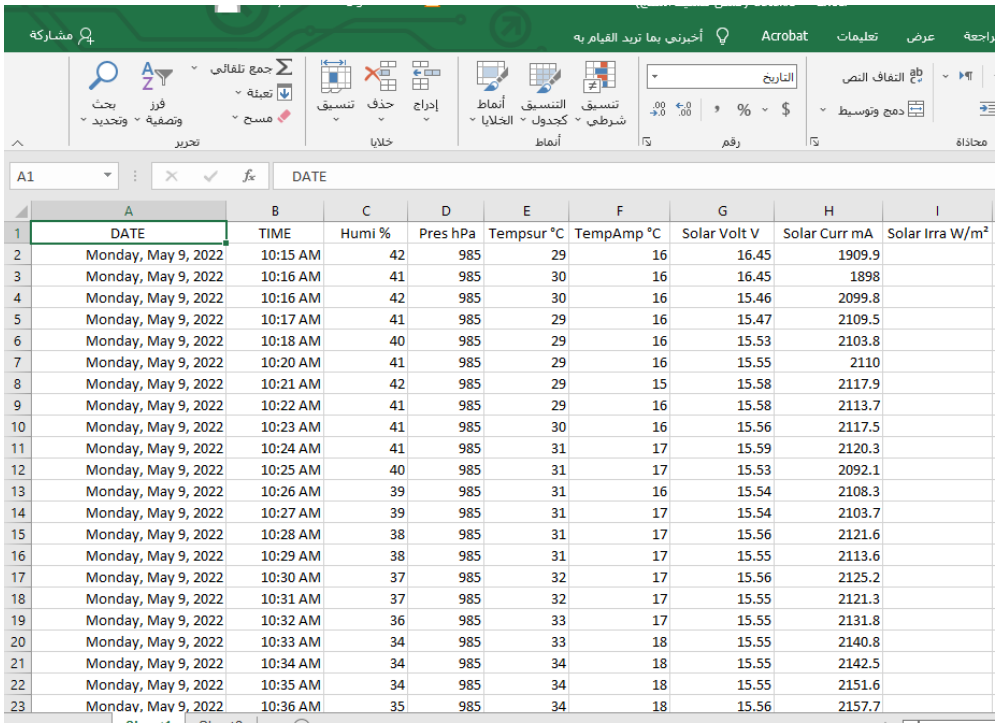

	A	B	C	D	E	F	G	H	I
1	DATE	TIME	Humi %	Pres hPa	Tempsur °C	TempAmp °C	Solar Volt V	Solar Curr mA	Solar Irra W/m²
2	Monday, May 9, 2022	10:15 AM	42	985	29	16	16.45	1909.9	
3	Monday, May 9, 2022	10:16 AM	41	985	30	16	16.45	1898	
4	Monday, May 9, 2022	10:16 AM	42	985	30	16	15.46	2099.8	
5	Monday, May 9, 2022	10:17 AM	41	985	29	16	15.47	2109.5	
6	Monday, May 9, 2022	10:18 AM	40	985	29	16	15.53	2103.8	
7	Monday, May 9, 2022	10:20 AM	41	985	29	16	15.55	2110	
8	Monday, May 9, 2022	10:21 AM	42	985	29	15	15.58	2117.9	
9	Monday, May 9, 2022	10:22 AM	41	985	29	16	15.58	2113.7	
10	Monday, May 9, 2022	10:23 AM	41	985	30	16	15.56	2117.5	
11	Monday, May 9, 2022	10:24 AM	41	985	31	17	15.59	2120.3	
12	Monday, May 9, 2022	10:25 AM	40	985	31	17	15.53	2092.1	
13	Monday, May 9, 2022	10:26 AM	39	985	31	16	15.54	2108.3	
14	Monday, May 9, 2022	10:27 AM	39	985	31	17	15.54	2103.7	
15	Monday, May 9, 2022	10:28 AM	38	985	31	17	15.56	2121.6	
16	Monday, May 9, 2022	10:29 AM	38	985	31	17	15.55	2113.6	
17	Monday, May 9, 2022	10:30 AM	37	985	32	17	15.56	2125.2	
18	Monday, May 9, 2022	10:31 AM	37	985	32	17	15.55	2121.3	
19	Monday, May 9, 2022	10:32 AM	36	985	33	17	15.55	2131.8	
20	Monday, May 9, 2022	10:33 AM	34	985	33	18	15.55	2140.8	
21	Monday, May 9, 2022	10:34 AM	34	985	34	18	15.55	2142.5	
22	Monday, May 9, 2022	10:35 AM	34	985	34	18	15.55	2151.6	
23	Monday, May 9, 2022	10:36 AM	35	985	34	18	15.56	2157.7	

Figure 3.11. Dataset logger file (data.csv).

The system operates automatically for 12 hours a day, from 7 am to 7 pm and data are taken every 1 minute.

SECTION 4

NEURAL NETWORK WITH OTHER ALGORITHMS

In this section, we are going to introduce the three main implemented algorithms: Genetic algorithm, Particle swarm optimization and Artificial bee colony. The basic idea is how each of these algorithms will help neural network to get high accuracy prediction of PV output.

4.1. Genetic Algorithm

The genetic algorithm (GA) is a branch of learning algorithms which cross over the ideas of biases and weights of two good neural networks; the crossing produces the best neural network with optimal biases and weights. GAs often provide the best solutions which reveal valuable insights about a problem.

4.1.1. Concept of GA working

Suppose an agent with weights needs to be optimized; initially, groups of random values of biases and weights are generated. This stage refers to neural networks as the first agent. Many tests are evaluated by the agent. The agent produces the result of the tests as a score. It repeats those many times to generate a population. It chooses the top 10% of the population to be used later by the crossover. Whenever crossover happens, mutations might occur. GA needs a cost function to be reduced. When this cost function reaches its minimum, the tested weights are the optimal values for the tested agent. This is GA with simple use. This process will slowly optimize the accuracy and performance. In our case, the agent was a neural network with weights needing to be optimized for better model performance.

Figure 4.1 shows the process of the GA with an agent (NN). In our case the cost function is Mean Square Error.

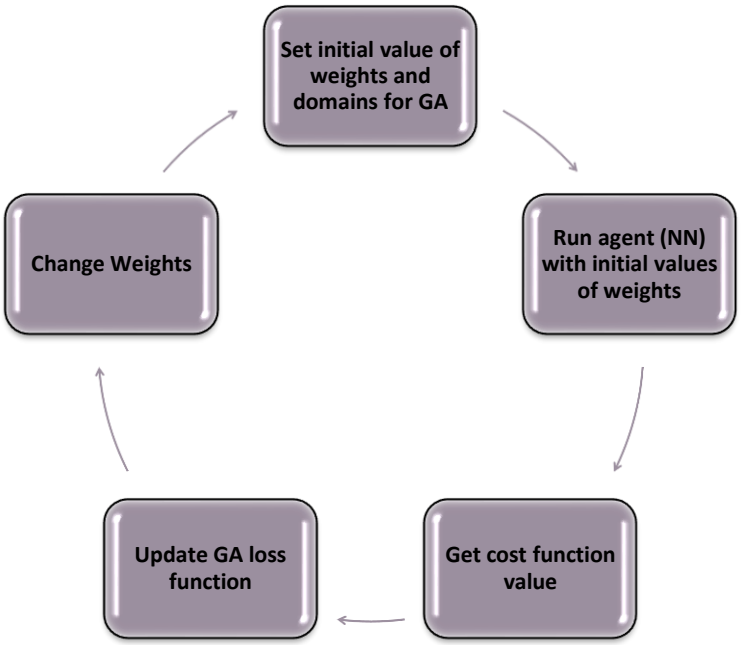

Figure 4.1. Loop of GA.

4.1.2. Advantages and disadvantages:

There are many advantages of Genetic Algorithms: a large domain of solutions, working on parallelism, simply needs less details about problem, solutions are multiple, global optimization.
Disadvantages of Genetic Algorithms: it requires special definitions for its parameters. Its calculation complexity.

4.1.3. GA vs ordinary algorithms

- In GA, the term "domain of searching" refers to the collection of all possible answers to the problem at hand. As opposed to Genetic Algorithms, which use several groups within a search area, conventional algorithms only keep one.
- Ordinary Algorithms need more details to achieve searching while Genetic Algorithms need only cost formula to compute the fitness of an individual solution.
- Ordinary Algorithms are not able to work on parallelism while GA has ability to do that (fitness function is calculated of each individual independently).

- Ordinary Algorithms will result in only one solution for the optimization problem, while Genetic Algorithms will give multiple optimal solutions from different generations.
- GA are stochastic and probabilistic, while traditional algorithms are predictable.
- GA has ability to handle multimodal problems.

Real-life applications of Genetic Optimization

- Traveling salesman problem (TSP)
- Vehicle routing problem (VRP)
- Financial markets.
- Manufacturing system.
- Mechanical engineering design.
- Data clustering and mining.
- Image processing.
- Neural networks.

In our study, Neural network is used to predict the solar power output with weight optimal selection using Genetic Algorithms.

4.2. Particle Swarm Optimization (PSO)

PSO is a computation technique which can be used to optimize a problem by iteratively trying to enhance a proposed solution with regard to a given quality metric (cost function). PSO works to optimize the best selection of parameters by defining candidate solutions as populations for these parameters, and then moving these particles in a search space counting on mathematic formulas by changing the particle's location and velocity. The motion of each particle is affected by its better location and is driven to achieve the best position in the search-space; the best positions are updated

PSO was original defined in [126] as a stylized representation of the motion of organisms in a bird flock or fish school. PSO does not guarantee finding the best solution. More specifically, PSO does not depend on the error gradient, optimization

is performed compared with ordinary optimization techniques such as gradient descent and quasi-Newton methods. PSO is used for optimization issues that are partially noisy, irregular, changeable with respect to time, etc.

4.2.1. Concept of PSO

The basics of the PSO algorithm are that it works depending on a population (named as a swarm) of candidate solutions (named particles). These particles change positions from current position to new positions around the search space. The process is repeated with the hope of finding a satisfactory solution; however, this is not guaranteed. Figure 4.2 shows the basic of PSO.

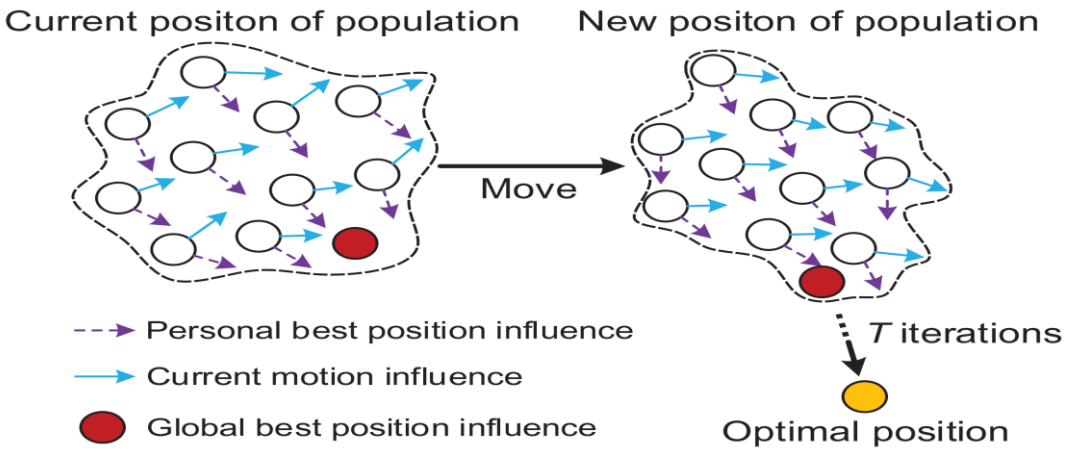

Figure 4.2. basic PSO diagram [127].

Formally, let f: $\mathbb{R}^n \rightarrow \mathbb{R}$ be the objective function which must be decreased. The function has an input a vector of candidate solution of real numbers and outputs a real number as value of the cost function to be minimized. The gradient of $\boldsymbol{f}$ is not known. The aim is to find a position in the space (solution) $\boldsymbol{a}$ for which $\boldsymbol{f}(\boldsymbol{a}) \leq \boldsymbol{f}(\boldsymbol{b})$ for all $\boldsymbol{b}$ in the search-space, the position $\boldsymbol{a}$ is the global minimum. Cost function might be in a form of $\boldsymbol{h} = -\boldsymbol{f}$, thus we need to maximize the function instead of minimizing it.

Let $\boldsymbol{S}$ be the total count of particles in the swarm; every particle has its own position and velocity $\boldsymbol{x_i} \in \mathbb{R}^n$ and $\boldsymbol{v_i} \in \mathbb{R}^{\boldsymbol{n}}$. Let $\boldsymbol{p}_i$ be the optimal position of particle $\boldsymbol{i}$, and let $\boldsymbol{g}$ be the optimal position of the entire swarm. A basic PSO algorithm is then:

- For every particle $\boldsymbol{i} = \mathbf{1}, \ldots, \boldsymbol{S}$, perform the following steps:
    - Start with the position of a particle by a random vector with uniform distribution: $\boldsymbol{x_i} \sim U(\boldsymbol{b_{lo}}, \boldsymbol{b_{up}})$, where $\boldsymbol{b_{up}}$ and $\boldsymbol{b_{lo}}$ are the upper boundary and lower boundaries of the search space, respectively;
    - Set the initial value of the particle's best position to: $\boldsymbol{p_i} \leftarrow \boldsymbol{x_i}$;
    - When $(f(\boldsymbol{p_i}) < f(\boldsymbol{g}))$, change $\boldsymbol{g} \leftarrow \boldsymbol{p_i}$;
    - Set the initial value of the particle's velocity: $\boldsymbol{v_i} \sim \boldsymbol{U}(-|\boldsymbol{b_{up}} - \boldsymbol{b_{lo}}|, |\boldsymbol{b_{up}} - \boldsymbol{b_{lo}}|)$.
- Until a termination condition is met (i.e., the final iteration is met, or a solution with adequate objective function value is found) :
    - For every particle $\boldsymbol{i} = \mathbf{1}, \ldots, \boldsymbol{S}$, perform the following steps:
        - Choose random numbers: $\boldsymbol{r_p}, \boldsymbol{r_g} \sim \boldsymbol{U}(\mathbf{0}, \mathbf{1})$;
        - For every $\boldsymbol{d} = \mathbf{1}, \ldots, \boldsymbol{n}$, perform the following steps:
        - Update the velocity of the particle;
        - Update the position of particle: $\boldsymbol{x_i} \leftarrow \boldsymbol{x_i} + \boldsymbol{Time} * \boldsymbol{v_i}$.
        - When $(\boldsymbol{f}(\boldsymbol{x_i}) < \boldsymbol{f}(\boldsymbol{p_i}))$, perform the following steps:
        - Update the best-known position of the particle: $\boldsymbol{p_i} \leftarrow \boldsymbol{x_i}$;
        - When $(\boldsymbol{f}(\boldsymbol{x_i}) < \boldsymbol{f}(\boldsymbol{g}))$, update the best-known position of the swarm: $\boldsymbol{g} \leftarrow \boldsymbol{p_i}$.
- Now **g** represents the best-found solution.

In our project, the PSO attempted to find optimal values of ANN weights.

4.3. Artifical Bee Colony (ABC)

The artificial bee colony (ABC) is an optimization algorithm that depends on the intelligent foraging behavior of a honeybee swarm. The ABC algorithm is a swarm-based meta-heuristic algorithm; it was first introduced by Karaboga in 2005 [128] to optimize numeric problems. The main idea was inspired by the smart searching of honeybees.

The algorithm specifically depends on the model proposed by Tereshko and Loengarov [129] for searching methods performed by bee colonies. The basic structure

contains three important parts: unemployed foraging bees; employed foraging bees; and food sources.

The role of the first two parts is to search for rich sources of food (third part) close to the hive. The structure also defines smart stages of leading of behavior; leading methods are very important for organization and how to collect food. The two stages are:

- The mobilization of foragers to find and retrieve rich sources of food, which is reconsidered as positive feedback;
- Foragers neglecting poor food sources, leading to negative feedback.

In summary, ABCs have bees which are named agents; these are smart forager bees with a problem to solve, i.e., smartly finding sources of rich food. To implement ABCs for any problem, we must convert the optimization problem into a problem of finding a solution in the form of searching for the best parameters that make cost functions as minimal as possible. As a result, the agents (smart bees) randomly find some initial solutions for the parameters, and then enhance the parameters iteratively using the following technique: moving to better positions by means of a neighbor search mechanism while abandoning poor solutions.

A global optimization problem can be defined as finding parameters as an array of one dimension, x, which minimizes the cost function f(x):

$$min\ f(x), \qquad x = (x_1, x_2, \dots, x_i, \dots, x_{n-1}, x_n) \in R^n \tag{4.1}$$

It has some constraints, as follows:

$$l_i \le x_i \le u_i, \ \ i = 1, \dots, n \tag{4.2}$$

subject to:

$$g_j(x) \le 0, for\ \ j = 1, \dots, p \tag{4.3}$$

$$h_j(x) = 0, for\ \ j = p+1, \dots, q \tag{4.4}$$

$f(x)$ is defined on a search space, $\boldsymbol{S}$, which has dimensions of n in R^n ($S \subseteq R^n$). There are limits for each variable, lower and upper: l_i and u_i, respectively.

This problem is also known as a constrained optimization problem. If it is an unconstrained optimization problem, then both $p = 0$ and $q = 0$.

4.3.1. The artificial bee colony meta-heuristic

In ABC, there are three groups of bees:

- Employed: which are associated with finding specific sources of food;
- Onlookers: which watch the movements of Employed bees in the hive to select sources of foods;
- Scouts: which randomly look for sources of food.

Scouts and onlookers are also called Unemployed bees. Initially, Scout bees work to find all food source positions. Thereafter, Onlooker bees and Employed bees test the nectar of food sources that are discovered by Scout bees. This is a continuous process until all sources are exhausted. Employed bees whose food sources have been exhausted become Scout bees. In ABCs, the location of food sources is a potential solution, and the quantity of nectar in this source considers the quality (fitness) of the solution.

The general flowchart of the ABC method is as follows:

REPEAT
    Employed Bees Phase
    Onlooker Bees Phase
    Scout Bees Phase
    Memorize the best solution achieved so far
UNTIL(Cycle = Maximum Cycle Number)

4.3.2. phase of initialization

All necessary parameters are initialized with random values as follows (m=1…m, m: $population\ size$) by scout bees, and the control parameters are set.

The following definition might be used for initialization purposes:

$$x_{mi} = l_i + rand(0,1) * (u_i - l_i) \tag{4.5}$$

Where l_i and u_i are the lower and upper bounds of parameter x_{mi} , respectively.

4.3.3. Employed bees phase

Employed bees search for new food sources (υ_m) with the condition of finding more nectar within the neighborhood of the food source x_{mi} in their memory. After they find a source of food, they check its quality (fitness). They might choose a neighbor source of food υ_m by the following formula:

$$\upsilon_{mi} = x_{mi} + \phi_{mi}(x_{mi} - x_{ki}) \tag{4.6}$$

Where x_{ki} is a randomly chosen source, i is also selected randomly, and ϕ_{mi} is a random term in the range $[-a, a]$. The quality value of the solution, $F_m(x_m)$, can be calculated to minimize problems using the subsequent equation:

$$F_m(x_m) = \begin{cases} \dfrac{1}{1 + F_m(x_m)} & if \quad F_m(x_m) \geq 0 \\ 1 + abs\big(F_m(x_m)\big) & if \quad F_m(x_m) \leq 0 \end{cases} \tag{4.7}$$

F_m a measure of something like the solution′s goal function′s x_m.

4.3.4. Onlooker bees phase

Smart Employed bees share information details about sources of food with smart Onlooker bees which are waiting in the hive. Smart Onlooker bees use the shared information with probabilities from the fitness function Fm to choose their food sources. Fitness-based selection methods might be used, such as the roulette wheel selection method [130].

The probability p_m that explains which x_m should be chosen can be calculated by:

$$p_m = \frac{F_m(x_m)}{\sum_{m=1}^{M} F_m(x_m)} \tag{4.8}$$

After Onlooker bees choose the location of food x_m, a neighborhood source, v_m, is defined by Equation (4.6) and its performance is calculated. It is in a phase of Employed bees; therefore, greedy selection is applied between v_m and x_m.

4.3.5. Scout bees phase

Solutions of Employed bees cannot be enhanced by a specific number of tries, defined by the user of the ABC algorithm and called "abandonment condition". Then, the converted Scouts begin to find new solutions. If solution x_m is being abandoned, the new solution is found by Scouts which were previously Employed bees of x_m, as be calculated by Equation (4.5). Hence, those sources which are initially poor or have been made poor by exploitation are abandoned, and negative feedback behavior arises to balance the positive feedback. Figure 4.3 displays the ABC flowchart.

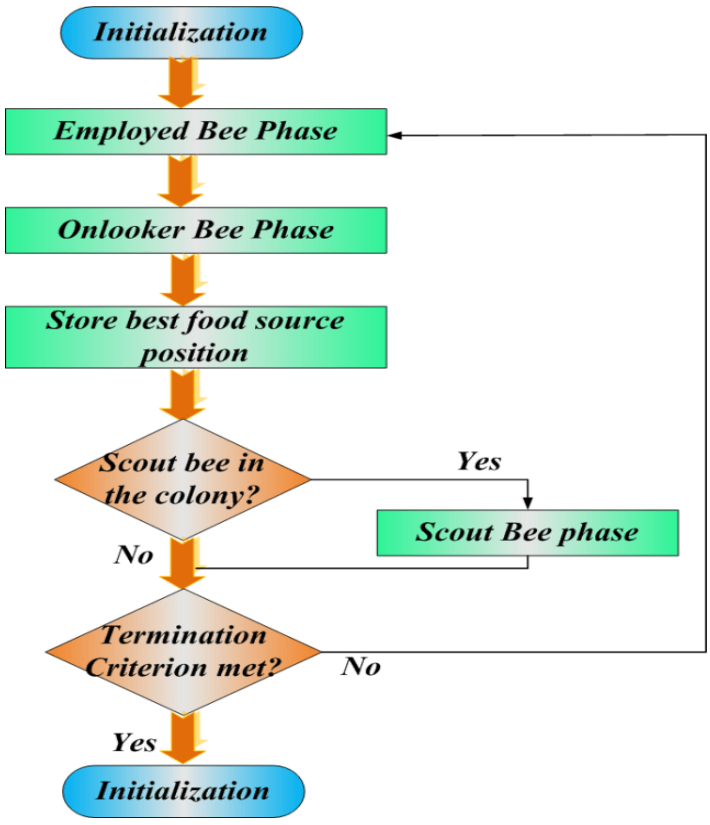

Figure 4.3. ABC flowchart.

.4.4. Validation Metrics

Suppose a vector of real values $\boldsymbol{Y}$ and a vector $\widehat{\mathbf{Y}}$ as predicted values of $\boldsymbol{Y}$. The length of vectors is N.

4.4.1. Mean square error

$$\boldsymbol{MSE} = \frac{\mathbf{1}}{\boldsymbol{N}}\sum_{\boldsymbol{i=1}}^{\boldsymbol{N}}\left(\boldsymbol{Y_i} - \widehat{\mathbf{Y}}_{\boldsymbol{i}}\right)^{\mathbf{2}} \tag{4.9}$$

4.4.2. Mean absolute percentage error

$$\boldsymbol{MAPE} = \frac{\mathbf{1}}{\boldsymbol{N}}\sum_{\boldsymbol{i=1}}^{\boldsymbol{N}}\left|\frac{\boldsymbol{Y_i} - \widehat{\mathbf{Y}}_{\boldsymbol{i}}}{\boldsymbol{Y_i}}\right| \tag{4.10}$$

4.4.3. Coefficient of determination $\boldsymbol{R^2}$

$$\boldsymbol{R^2} = \mathbf{1} - \frac{\boldsymbol{RSS}}{\boldsymbol{TSS}} \tag{4.-11}$$

RSS: residual sum of squares, TSS: total sum of squares.

$$\boldsymbol{RSS} = \sum_{\boldsymbol{i=1}}^{\boldsymbol{N}}\left(\boldsymbol{Y_i} - \widehat{\mathbf{Y}}_{\boldsymbol{i}}\right)^{\mathbf{2}} \tag{4.-12}$$

$$\boldsymbol{TSS} = \sum_{\boldsymbol{i=1}}^{\boldsymbol{N}}(\boldsymbol{Y_i} - \overline{\boldsymbol{Y}})^{\mathbf{2}} \tag{4.-13}$$

$\overline{\boldsymbol{Y}}$ is the mean of $\boldsymbol{Y_i}$

SECTION 5

IMPLEMENTATIONS AND RESULTS

5.1. Data Processing

The data are measured in the study: 'DATE', 'TIME', 'Humidity', 'Pressure', 'Tempsur', 'TempAmp', 'SolarV', 'SolarC', 'SolarIr', and 'SolarP'. The label of data is the last column 'SolarP'. Other columns were gathered as the features or inputs for the tested algorithm. The prediction accuracy of all data has been improved in different weather conditions.

The setup for all methods is shown below:

For GA: Tolerance function: $1 * 10^{-10}$, number of generations: 200, cost function desired limit $1 * 10^{-7}$.

For PSO: Personal learning coefficient: 0.8, population size: 150, iterations: 500, range of values [–5,5].

For ABC: Tolerance function: $1 * 10^{-8}$, iterations: 1000.

5.2. Traditional ANN

We define the number of neurons as 18; ANN is a traditional feedforward network.

As shown in Figure 5.1 and Figure 5.2, the final error is around "0".

During training, the error is 0.0252%. The error gradient is about "0.0001".

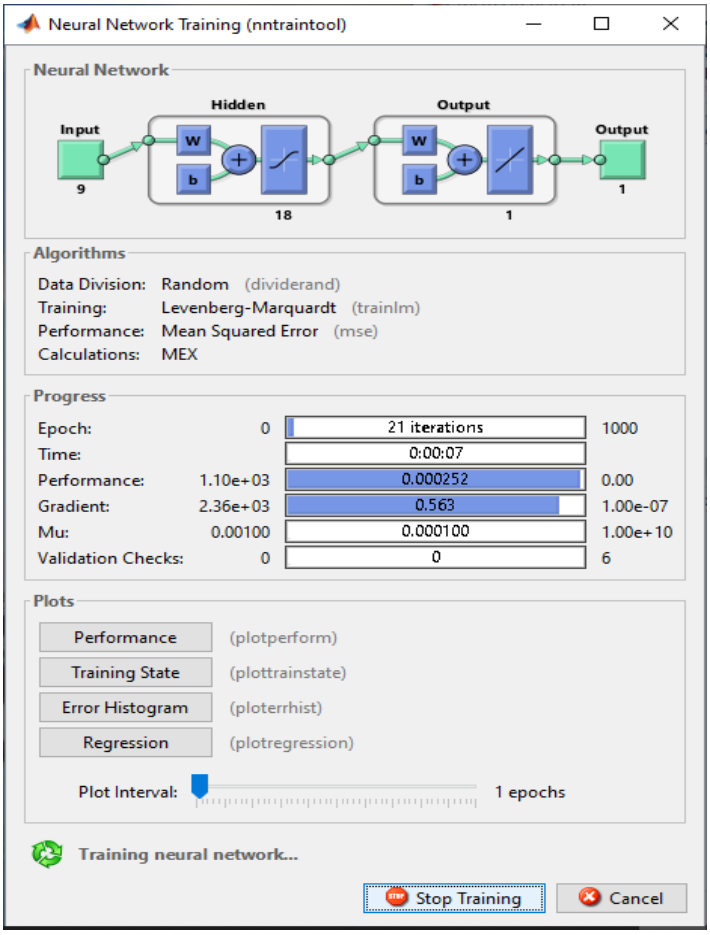

Figure 5.1. Training process.

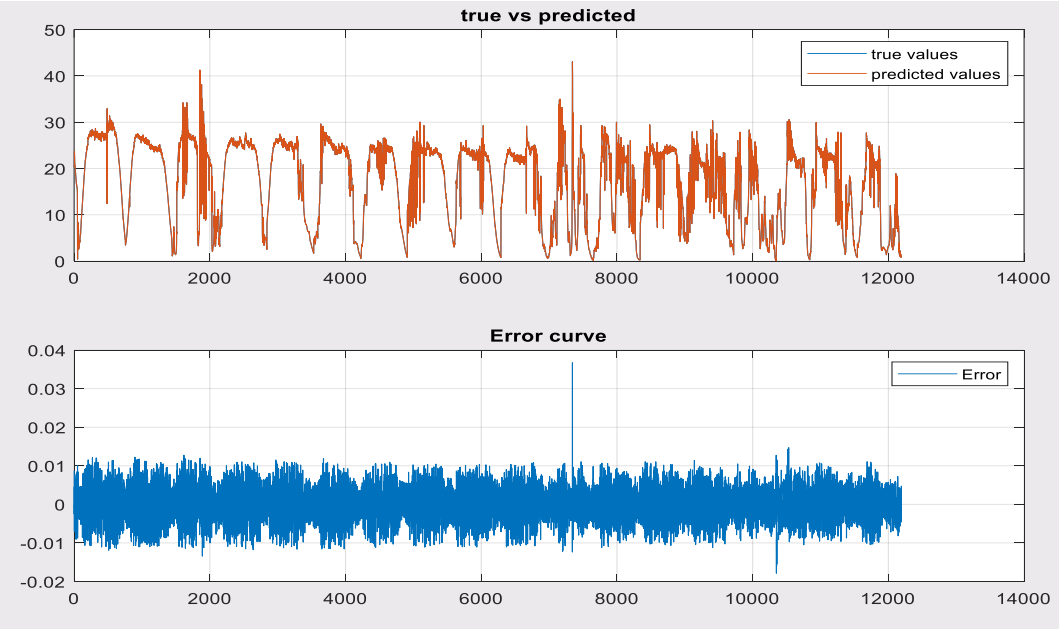

Figure 5.2. ANN results on real data.

Figure 5.2 shows the neural network results. The true values and predicted values are the same and errors around “0” with “mean 0” and standard deviation is “0.1”. It can be shown that there are 18 neurons in hidden layer of network and there are 9 features as input. It is shown in Figure 5.3.

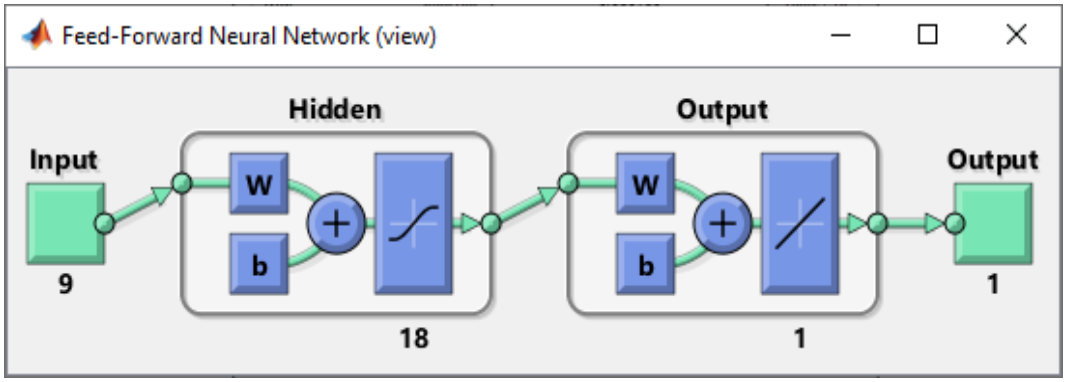

Figure 5.3. The ANN.

The performance when NN ends training is shown in Figure 5.4. It reached about ”0.0005”.

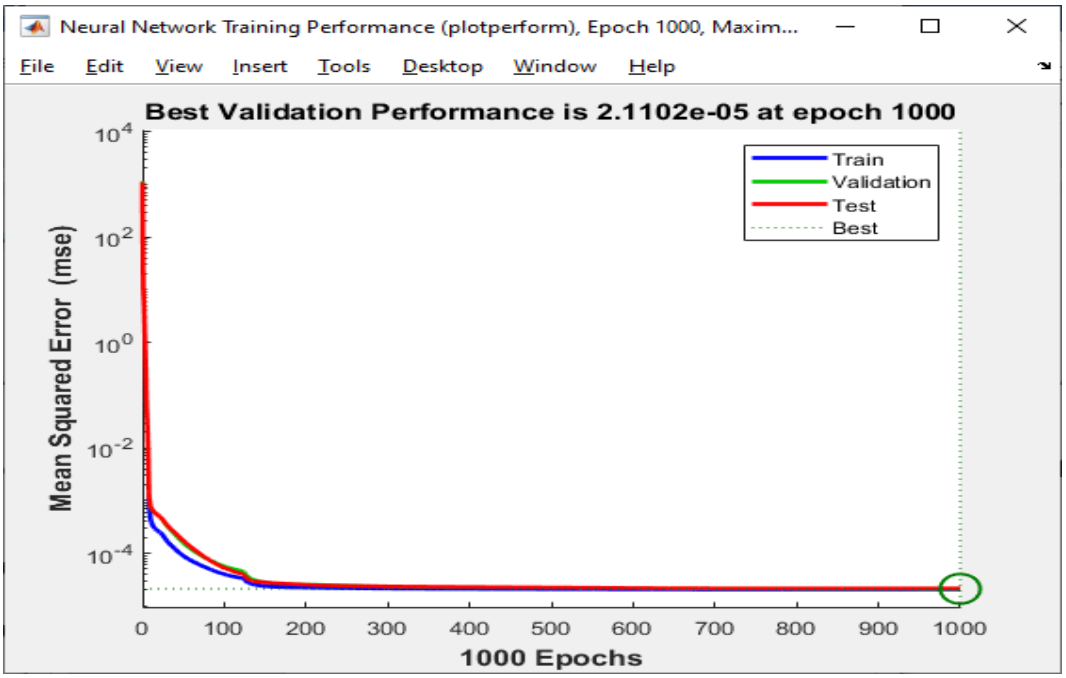

Figure 5.4. Traditional ANN performance.

Now let us test the Genetic algorithm with Neural network.

5.3. ANN with Genetic Algorithm

We define the same network as previous with 18 neurons. Then we get the weights from the ANN and define the GA options:

ga_opts = gaoptimset('PopInitRange', [-2;2], 'TolFun', 1e-10,'display','iter');

ga_opts = gaoptimset(ga_opts, 'StallGenLimit', 100, 'FitnessLimit', 1e-5, 'Generations', 200);

Number of generations is 200 and initial range for population is [-2, +2], with minimum value of fitness function and tolerance function. We pass the weights as input for GA and cost function is Mean Square Error. If the objective function does not improve within a period of time equal to the Stall time limit ('StallGenLimit') in seconds, the algorithm terminates. Table 5.1 depicts the procedure in detail.

Table 5.1. The cost function process of the GA–ANN.

Generation	Best Cost Function	Mean Cost Function
1	10.61	445.6
2	10.61	617.2
3	10.61	725.2
4	10.61	726.6
5	10.61	819.7
6	10.61	896.7
7	10.61	795.7
8	10.61	753.2
9	10.61	771.9
10	10.61	761.1
11	9.497	834.7
12	9.464	828.7
13	9.438	775.7
14	7.963	733.7
15	7.518	772.8

The process output shows that many iterations the best fitness cost function is decreased. The final results are shown in Figure 5.5. and Figure 5.6. at second test.

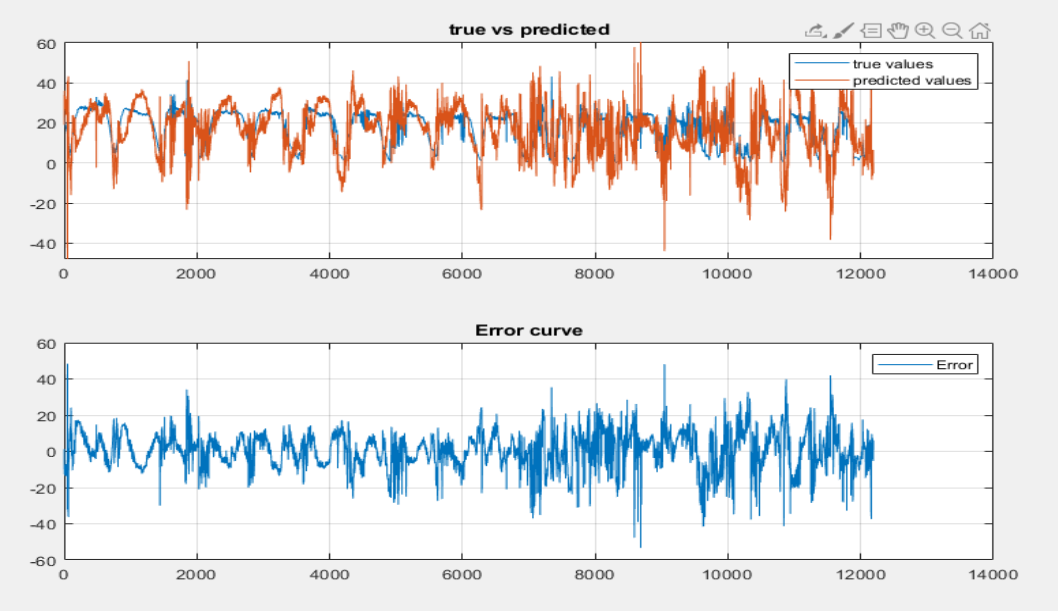

Figure 5.5. GA-ANN results (first test).

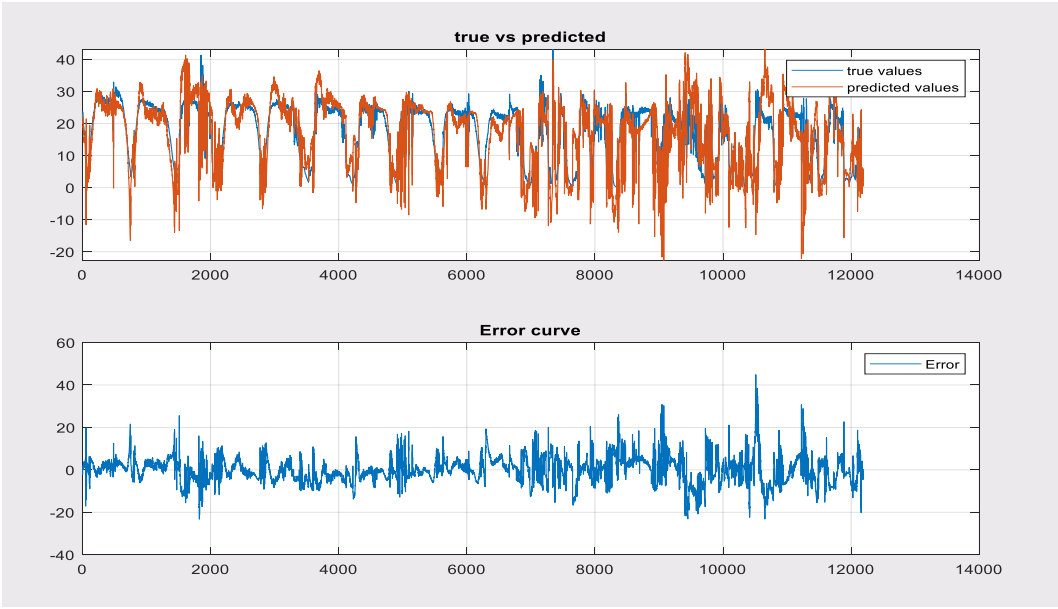

Figure 5.6. GA-ANN results (second test).

According to second test, the mean error is around 0 and standard deviation is less than 10, it can be seen that it is bad algorithm.

5.4. ANN with PSO

Table 5.2 shows changes in the first 10 epochs.

Table 5.2. Best function during the process of the PSO–ANN.

Iteration	Best Cost Function
1	43.4098
2	43.4098
3	18.8759
4	1.368
5	1.368
6	1.368
7	1.368
8	1.368
9	1.368
10	1.368

The process output shows that after many iterations the best fitness cost function is decreased. It reached “0.005” after 500 iterations. The cost function is shown in Figure 5.7.

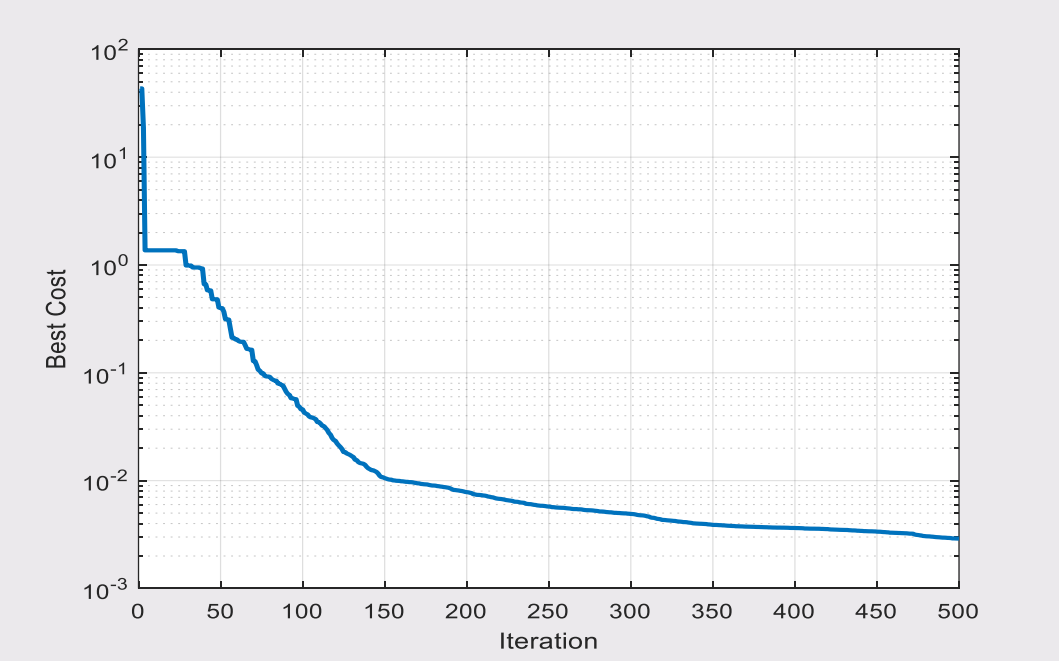

Figure 5.7. PSO-ANN cost function.

Figure 5.8 displays the results.

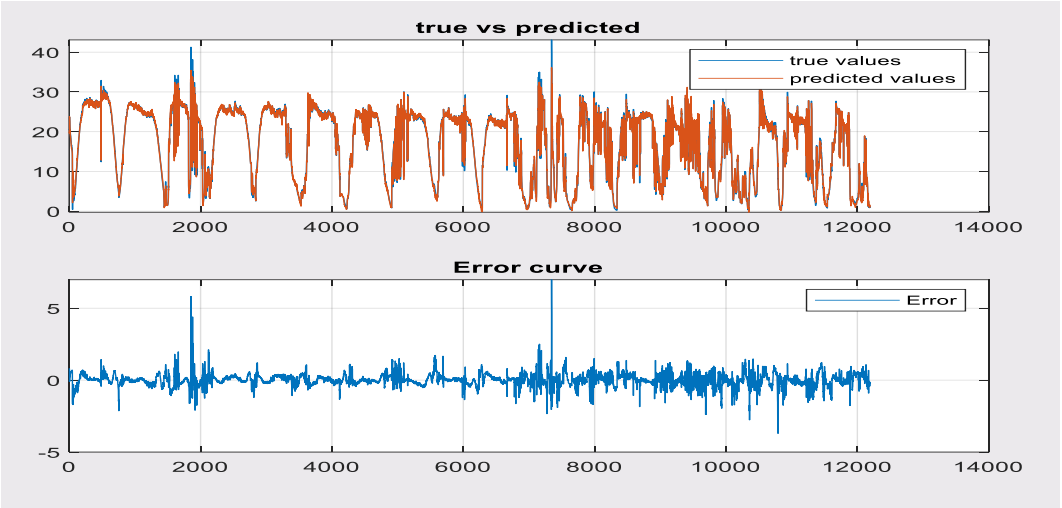

Figure 5.8. PSO-ANN results.

According to previous results, the mean error is around “0” and standard deviation is less than “2.5”. It can be seen that it is a good algorithm.

5.5. ANN with ABC

In this algorithm, splitting dataset was implemented. Data set was split into test and train part. The results are shown in Figure 5.9 as test part and Figure 5.10 as train part.

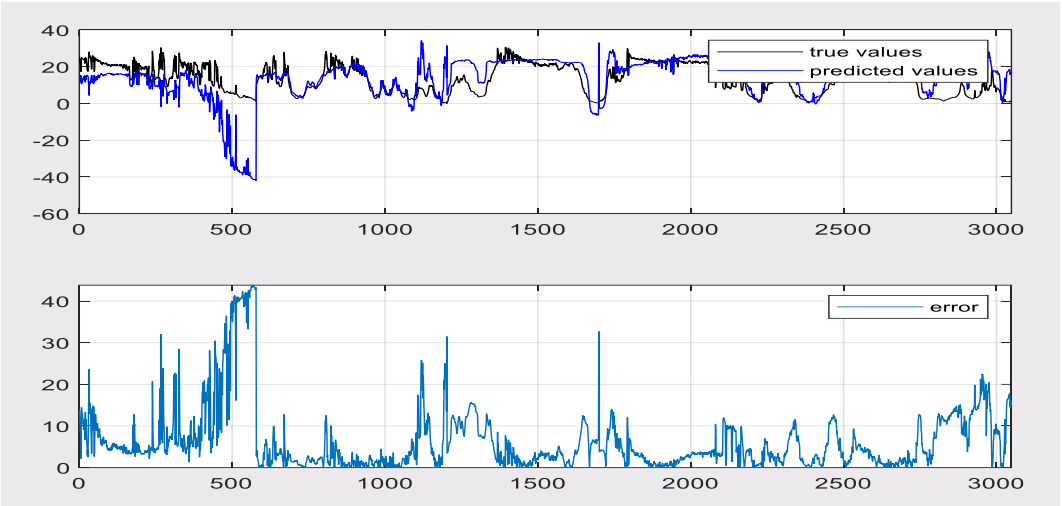

Figure 5.9. ABC-ANN for testing part.

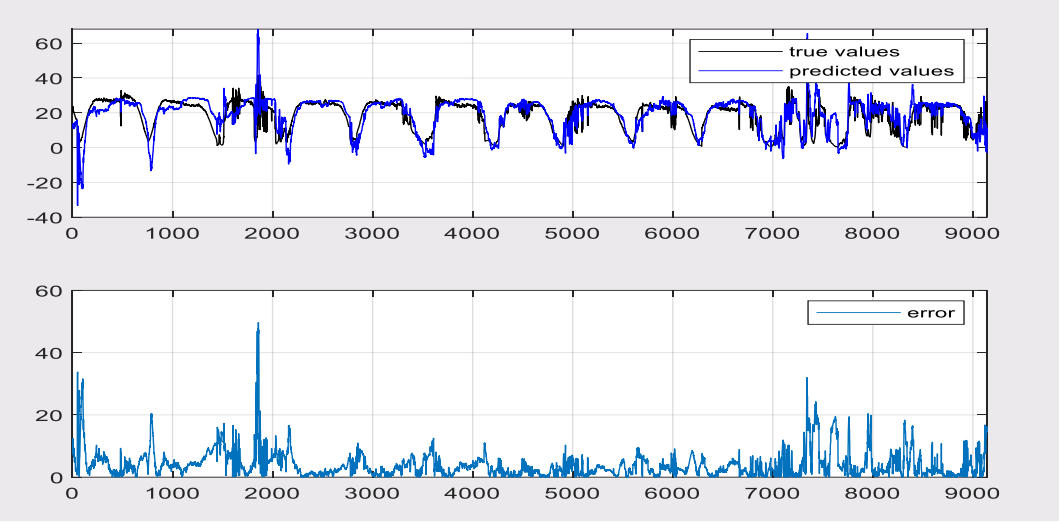

Figure 5.10. ABC-ANN for training part.

5.6. Results Comparisons

The fitness function is Normalized Mean Square Error (NMSE) for all methods. The citeria for GA is global minimum. The solution found by PSO is quite close to the global optimal. ABS is also searching for global minimum.

All methods are compared in Table 5.3.

Table 5.3. Table of comparison.

	MSE	MAPE	R^2
Traditional ANN	0.000020349	0.00040514	1
GA-ANN	6.1440	0.6790	0.4841
PSO-ANN	0.4607	0.0524	0.9971
ABC-ANN	35.1428	0.7890	0.5004

The results show that the traditional NN with basic finding methods is the best. PSO–ANN is the best between PSO–ANN, GA–ANN and ABC–ANN. Each study has its own dataset, the comparison would not be valuable because it is not the same dataset. However, we can tell that our methods have achieved a great accuracy, especially PSO-ANN, since the accuracy was 99.71%. The dataset can be shared with other researchers to obtain a comparison in the future.

SECTION 6

CONCLUSION AND FUTURE SCOPES

6.1. Conclusion

DAS system was developed at Karabuk University and contains the sensors for obtaining environment and electrical parameters and archiving the site via SD card data logger and saving the data on an excel file, and the other branch is in the laboratory, which is used for archiving and monitoring data via the locally and IOT by ThingSpeak.

In this work, implementation for solar power output predicting was performed with ANN and three different optimization algorithms: genetic algorithm, particle swarm optimization and artificial bee colony. Each method has been ran more than 10 times and results were monitored. The results showed that the PSO is best algorithm for finding optimal parameters of ANNs. Its performance (with respect to R^2) was 99.71% with minimum MSE and MAPE values. In the future, these algorithms can be analyzed and more details about their parameters can be determined. Utilizing more features of the datasets can also enhance the model of prediction.

6.2. Future Scopes

New optimization algorithms can be implemented and tested for future scopes. However, by changing the parameters used as inputs for the ANN algorithm, different features in the study can be tested and the effect of the inputs on the final results can be investigated. Separating the dataset into steady, sunny, and cloudy groups can help increase the forecast's precision.

REFERENCES

[1] Ü. Başaran Filik, T. Filik, and Ö. Nezih Gerek, "New electric transmission systems: experiences from Turkey," *Handb. Clean Energy Syst.*, pp. 1–13, 2015.

[2] B. Zazoum, "Solar photovoltaic power prediction using different machine learning methods," *Energy Reports*, vol. 8, pp. 19–25, 2022, doi: 10.1016/j.egyr.2021.11.183.

[3] A. El Hendouzi and A. Bourouhou, "Solar Photovoltaic Power Forecasting," *J. Electr. Comput. Eng.*, vol. 2020, 2020, doi: 10.1155/2020/8819925.

[4] B. Nordell, "Thermal pollution causes global warming," *Glob. Planet. Change*, vol. 38, no. 3–4, pp. 305–312, 2003, doi: 10.1016/S0921-8181(03)00113-9.

[5] H. Eroğlu, "Effects of Covid-19 outbreak on environment and renewable energy sector," *Environ. Dev. Sustain.*, vol. 23, no. 4, pp. 4782–4790, 2021.

[6] K. Das, "Impact of COVID-19 pandemic into solar energy generation sector," *Available SSRN 3580341*, 2020.

[7] S. Halbrügge, P. Schott, M. Weibelzahl, H. U. Buhl, G. Fridgen, and M. Schöpf, "How did the German and other European electricity systems react to the COVID-19 pandemic?," *Appl. Energy*, vol. 285, p. 116370, 2021.

[8] M. Vaka, R. Walvekar, A. K. Rasheed, and M. Khalid, "A review on Malaysia's solar energy pathway towards carbon-neutral Malaysia beyond Covid'19 pandemic," *J. Clean. Prod.*, vol. 273, p. 122834, 2020.

[9] K. T. Gillingham, C. R. Knittel, J. Li, M. Ovaere, and M. Reguant, "The Short-run and Long-run Effects of Covid-19 on Energy and the Environment," *Joule*, vol. 4, no. 7, pp. 1337–1341, 2020.

[10] Y. Song, T. Liu, Y. Li, and B. Ye, "The influence of COVID-19 on grid parity of China's photovoltaic industry," *Environ. Geochem. Health*, pp. 1–16, 2020.

[11] A. Radu, C. E. Panaite, and A. Popescu, "Impact of COVID-19 pandemic on renewable sources implementation: case of PV systems in Romania," in *IOP Conference Series: Materials Science and Engineering*, 2020, vol. 997, no. 1, p. 12154.

[12] K. Peters, "COVID-19: How GOGLA is helping the off-grid solar industry deal with the crisis." https://www.gogla.org/about-us/blogs/covid-19-how-gogla-is-helping-the-off-grid-solar-industry-deal-with-the-crisis (accessed May 05, 2021).

[13] J. W. Burnett and F. Hefner, "Solar energy adoption: A case study of South Carolina," *Electr. J.*, vol. 34, no. 5, p. 106958, 2021.

[14] “Renewable Energy Market Update,” *Renew. Energy Mark. Updat.*, 2020, doi: 10.1787/afbc8c1d-en.

[15] I. E. Agency, “Renewables,” 2021.

[16] G. Ramkumar *et al.*, “A Short-Term Solar Photovoltaic Power Optimized Prediction Interval Model Based on FOS-ELM Algorithm,” *Int. J. Photoenergy*, vol. 2021, 2021, doi: 10.1155/2021/3981456.

[17] M. Yang and X. Huang, “An Evaluation Method of the Photovoltaic Power Prediction Quality,” *Math. Probl. Eng.*, vol. 2018, 2018, doi: 10.1155/2018/9049215.

[18] H. Jiang, L. Lu, and K. Sun, “Experimental investigation of the impact of airborne dust deposition on the performance of solar photovoltaic (PV) modules,” *Atmos. Environ.*, vol. 45, no. 25, pp. 4299–4304, 2011.

[19] A. Virtuani, D. Pavanello, and G. Friesen, “Overview of temperature coefficients of different thin film photovoltaic technologies,” in *25th European photovoltaic solar energy conference and exhibition/5th World conference on photovoltaic energy conversion*, 2010, vol. 4, pp. 3–83.

[20] E. Radziemska, “The effect of temperature on the power drop in crystalline silicon solar cells,” *Renew. energy*, vol. 28, no. 1, pp. 1–12, 2003.

[21] H. Bahaidarah, A. Subhan, P. Gandhidasan, and S. Rehman, “Performance evaluation of a PV (photovoltaic) module by back surface water cooling for hot climatic conditions,” *Energy*, vol. 59, pp. 445–453, 2013.

[22] J. Ekström, M. Koivisto, J. Millar, I. Mellin, and M. Lehtonen, “A statistical approach for hourly photovoltaic power generation modeling with generation locations without measured data,” *Sol. Energy*, vol. 132, pp. 173–187, 2016.

[23] S. Daliento *et al.*, “Monitoring, diagnosis, and power forecasting for photovoltaic fields: A review,” *Int. J. Photoenergy*, vol. 2017, 2017, doi: 10.1155/2017/1356851.

[24] M. Pi, N. Jin, D. Chen, and B. Lou, “Short-Term Solar Irradiance Prediction Based on Multichannel LSTM Neural Networks Using Edge-Based IoT System,” *Wirel. Commun. Mob. Comput.*, vol. 2022, 2022.

[25] Z. Cheng, Q. Liu, and W. Zhang, “Improved probability prediction method research for photovoltaic power output,” *Appl. Sci.*, vol. 9, no. 10, 2019, doi: 10.3390/app9102043.

[26] K. Hu, S. Cao, L. Wang, W. Li, and M. Lv, “A new ultra-short-term photovoltaic power prediction model based on ground-based cloud images,” *J. Clean. Prod.*, vol. 200, pp. 731–745, 2018.

[27] P. Li, K. Zhou, X. Lu, and S. Yang, “A hybrid deep learning model for short-term PV power forecasting,” *Appl. Energy*, vol. 259, p. 114216, 2020.

[28] Y. Jung, J. Jung, B. Kim, and S. Han, “Long short-term memory recurrent neural network for modeling temporal patterns in long-term power forecasting for solar PV facilities: Case study of South Korea,” *J. Clean. Prod.*, vol. 250, p. 119476, 2020.

[29] S. Han, Y. Qiao, J. Yan, Y. Liu, L. Li, and Z. Wang, “Mid-to-long term wind and photovoltaic power generation prediction based on copula function and long short term memory network,” *Appl. Energy*, vol. 239, pp. 181–191, 2019.

[30] H. Zhou, Y. Zhang, L. Yang, Q. Liu, K. Yan, and Y. Du, “Short-term photovoltaic power forecasting based on long short term memory neural network and attention mechanism,” *Ieee Access*, vol. 7, pp. 78063–78074, 2019.

[31] M. Santhosh, C. Venkaiah, and D. M. V. Kumar, “Short-term wind speed forecasting approach using ensemble empirical mode decomposition and deep Boltzmann machine,” *Sustain. Energy, Grids Networks*, vol. 19, p. 100242, 2019.

[32] U. K. Das *et al.*, “Forecasting of photovoltaic power generation and model optimization: A review,” *Renew. Sustain. Energy Rev.*, vol. 81, pp. 912–928, 2018.

[33] C. Voyant and G. Notton, “Solar irradiation nowcasting by stochastic persistence: A new parsimonious, simple and efficient forecasting tool,” *Renew. Sustain. Energy Rev.*, vol. 92, pp. 343–352, 2018.

[34] T. S. Nielsen, A. Joensen, H. Madsen, L. Landberg, and G. Giebel, “A new reference for wind power forecasting,” *Wind Energy An Int. J. Prog. Appl. Wind Power Convers. Technol.*, vol. 1, no. 1, pp. 29–34, 1998.

[35] M. Lipperheide, J. L. Bosch, and J. Kleissl, “Embedded nowcasting method using cloud speed persistence for a photovoltaic power plant,” *Sol. Energy*, vol. 112, pp. 232–238, 2015.

[36] M. Diagne, M. David, P. Lauret, J. Boland, and N. Schmutz, “Review of solar irradiance forecasting methods and a proposition for small-scale insular grids,” *Renew. Sustain. Energy Rev.*, vol. 27, pp. 65–76, 2013.

[37] X. Yang, J. Ren, and H. Yue, “Photovoltaic power forecasting with a rough set combination method,” in *2016 UKACC 11th International Conference on Control (CONTROL)*, 2016, pp. 1–6.

[38] A. Ahmad, T. N. Anderson, and T. T. Lie, “Hourly global solar irradiation forecasting for New Zealand,” *Sol. Energy*, vol. 122, pp. 1398–1408, 2015.

[39] A. Sanfilippo, L. Martin-Pomares, N. Mohandes, D. Perez-Astudillo, and D.

Bachour, “An adaptive multi-modeling approach to solar nowcasting,” *Sol. Energy*, vol. 125, pp. 77–85, 2016.

[40] L. Martín, L. F. Zarzalejo, J. Polo, A. Navarro, R. Marchante, and M. Cony, “Prediction of global solar irradiance based on time series analysis: Application to solar thermal power plants energy production planning,” *Sol. Energy*, vol. 84, no. 10, pp. 1772–1781, 2010.

[41] P. Lauret, C. Voyant, T. Soubdhan, M. David, and P. Poggi, “A benchmarking of machine learning techniques for solar radiation forecasting in an insular context,” *Sol. Energy*, vol. 112, pp. 446–457, 2015.

[42] C. Monteiro, L. A. Fernandez-Jimenez, I. J. Ramirez-Rosado, A. Muñoz-Jimenez, and P. M. Lara-Santillan, “Short-term forecasting models for photovoltaic plants: Analytical versus soft-computing techniques,” *Math. Probl. Eng.*, vol. 2013, 2013.

[43] A. Dolara, F. Grimaccia, S. Leva, M. Mussetta, and E. Ogliari, “A physical hybrid artificial neural network for short term forecasting of PV plant power output,” *Energies*, vol. 8, no. 2, pp. 1138–1153, 2015.

[44] M. Lei, L. Shiyan, J. Chuanwen, L. Hongling, and Z. Yan, “A review on the forecasting of wind speed and generated power,” *Renew. Sustain. energy Rev.*, vol. 13, no. 4, pp. 915–920, 2009.

[45] S. S. Soman, H. Zareipour, O. Malik, and P. Mandal, “A review of wind power and wind speed forecasting methods with different time horizons,” in *North American Power Symposium 2010*, 2010, pp. 1–8.

[46] G. Giebel, C. Draxl, R. Brownsword, G. Kariniotakis, and M. Denhard, “The state-of-the-art in short-term prediction of wind power. A literature overview,” 2011.

[47] A. Gandelli, F. Grimaccia, S. Leva, M. Mussetta, and E. Ogliari, “Hybrid model analysis and validation for PV energy production forecasting,” in *2014 international joint conference on neural networks (IJCNN)*, 2014, pp. 1957–1962.

[48] A. Ahmed and M. Khalid, “A review on the selected applications of forecasting models in renewable power systems,” *Renew. Sustain. Energy Rev.*, vol. 100, pp. 9–21, 2019.

[49] A. A. Ezzat, M. Jun, and Y. Ding, “Spatio-temporal asymmetry of local wind fields and its impact on short-term wind forecasting,” *IEEE Trans. Sustain. energy*, vol. 9, no. 3, pp. 1437–1447, 2018.

[50] R. Huang, T. Huang, R. Gadh, and N. Li, “Solar generation prediction using the ARMA model in a laboratory-level micro-grid,” in *2012 IEEE third international conference on smart grid communications (SmartGridComm)*,

2012, pp. 528–533.

[51] J. Boland, “Time series modeling of solar radiation. Modelling Solar Radiation at the Earthâ€™s Surface, V. Badescu.” Springer-Verlag Berlin Heidelberg, 2008.

[52] G. E. P. Box, G. M. Jenkins, G. C. Reinsel, and G. M. Ljung, *Time series analysis: forecasting and control*. John Wiley & Sons, 2015.

[53] W. K. A. Wan Ahmad and S. Ahmad, “Arima model and exponential smoothing method: A comparison,” in *AIP Conference Proceedings*, 2013, vol. 1522, no. 1, pp. 1312–1321.

[54] S. Pasari and A. Shah, “Time series auto-regressive integrated moving average model for renewable energy forecasting,” in *Enhancing Future Skills and Entrepreneurship*, Springer, Cham, 2020, pp. 71–77.

[55] S. Atique, S. Noureen, V. Roy, V. Subburaj, S. Bayne, and J. Macfie, “Forecasting of total daily solar energy generation using ARIMA: A case study,” in *2019 IEEE 9th annual computing and communication workshop and conference (CCWC)*, 2019, pp. 114–119.

[56] Y. Li, Y. Su, and L. Shu, “An ARMAX model for forecasting the power output of a grid connected photovoltaic system,” *Renew. Energy*, vol. 66, pp. 78–89, 2014.

[57] B. Keshtegar, C. Mert, and O. Kisi, “Comparison of four heuristic regression techniques in solar radiation modeling: Kriging method vs RSM, MARS and M5 model tree,” *Renew. Sustain. energy Rev.*, vol. 81, pp. 330–341, 2018.

[58] M. Abuella and B. Chowdhury, “Solar power probabilistic forecasting by using multiple linear regression analysis,” in *SoutheastCon 2015*, 2015, pp. 1–5.

[59] P. Lauret, M. David, and H. T. C. Pedro, “Probabilistic solar forecasting using quantile regression models,” *energies*, vol. 10, no. 10, p. 1591, 2017.

[60] G. Wang, Y. Su, and L. Shu, “One-day-ahead daily power forecasting of photovoltaic systems based on partial functional linear regression models,” *Renew. Energy*, vol. 96, pp. 469–478, 2016.

[61] M. N. Akhter, S. Mekhilef, H. Mokhlis, and N. M. Shah, “Review on forecasting of photovoltaic power generation based on machine learning and metaheuristic techniques,” *IET Renew. Power Gener.*, vol. 13, no. 7, pp. 1009–1023, 2019.

[62] R. Belu, “Artificial intelligence techniques for solar energy and photovoltaic applications,” in *Robotics: Concepts, methodologies, tools, and applications*, IGI Global, 2014, pp. 1662–1720.

[63] A. Mellit, S. A. Kalogirou, L. Hontoria, and S. Shaari, “Artificial intelligence techniques for sizing photovoltaic systems: A review,” *Renew. Sustain. Energy*

Rev., vol. 13, no. 2, pp. 406–419, 2009.

[64] P. Du, J. Wang, W. Yang, and T. Niu, "A novel hybrid model for short-term wind power forecasting," *Appl. Soft Comput.*, vol. 80, pp. 93–106, 2019.

[65] M. E. H. Chowdhury *et al.*, "Wearable real-time heart attack detection and warning system to reduce road accidents," *Sensors*, vol. 19, no. 12, p. 2780, 2019.

[66] M. E. H. Chowdhury *et al.*, "Real-time smart-digital stethoscope system for heart diseases monitoring," *Sensors*, vol. 19, no. 12, p. 2781, 2019.

[67] Y. Jiang, G. Huang, X. Peng, Y. Li, and Q. Yang, "A novel wind speed prediction method: Hybrid of correlation-aided DWT, LSSVM and GARCH," *J. Wind Eng. Ind. Aerodyn.*, vol. 174, pp. 28–38, 2018.

[68] E. Karami, M. Rafi, and A. Ridah, "Output PV power prediction using an artificial neural network in Casablanca, Morocco," in *Proceedings of the 4th International Conference on Smart City Applications*, 2019, pp. 1–8.

[69] A. Geetha *et al.*, "Prediction of hourly solar radiation in Tamil Nadu using ANN model with different learning algorithms," *Energy Reports*, vol. 8, pp. 664–671, 2022.

[70] A. T. Mohammad, Z. S. Al-Sagar, A. N. Hussain, and M. K. A. Al-Tamimi, "Prediction of PV Solar Panel Output Characteristics Using a Multilayer Artificial Neural Network (MLANN)," in *IOP Conference Series: Materials Science and Engineering*, 2021, vol. 1105, no. 1, p. 12013.

[71] S. Lopes, E. Cari, and S. Hajimirza, "A Comparative analysis of Artificial Neural Networks for Photovoltaic Power Forecast using remotes and local measurements," *J. Sol. Energy Eng.*, vol. 144, no. 2, 2022.

[72] M. Abuella and B. Chowdhury, "Solar power forecasting using artificial neural networks," in *2015 North American Power Symposium (NAPS)*, 2015, pp. 1–5.

[73] D. O'Leary and J. Kubby, "Feature selection and ANN solar power prediction," *J. Renew. Energy*, vol. 2017, 2017.

[74] C. G. Ozoegwu, "Artificial neural network forecast of monthly mean daily global solar radiation of selected locations based on time series and month number," *J. Clean. Prod.*, vol. 216, pp. 1–13, 2019.

[75] B. S. Bhaumik S., Chattopadhyay S., Chattopadhyay T., "An Artificial Intelligence Approach to the Prediction of Global Solar Irradiation in India," *Proc. Int. Conf. Ind. Instrum. Control*, vol. 815, no. 1876–1119, pp. 237–245, doi: https://doi.org/10.1007/978-981-16-7011-4_24.

[76] S. Hashunao, H. Sunku, and R. K. Mehta, "Modelling and Forecasting of Solar Radiation Data: A Case Study," in *Modeling, Simulation and Optimization*,

Springer, 2021, pp. 1–13.

[77] A. Yona, T. Senjyu, A. Saber, T. Funabashi, H. Sekine, and C. H. Kim, “Application of neural network to one-day-ahead 24h generating power forecasting for photovoltaic system.”

[78] H. Su, E. Zio, J. Zhang, M. Xu, X. Li, and Z. Zhang, “A hybrid hourly natural gas demand forecasting method based on the integration of wavelet transform and enhanced Deep-RNN model,” *Energy*, vol. 178, pp. 585–597, 2019.

[79] H. K. Ahn and N. Park, “Deep RNN-based photovoltaic power short-term forecast using power IoT sensors,” *Energies*, vol. 14, no. 2, p. 436, 2021.

[80] S. Hochreiter and J. Schmidhuber, “Long short-term memory,” *Neural Comput.*, vol. 9, no. 8, pp. 1735–1780, 1997.

[81] S. Hochreiter, “The vanishing gradient problem during learning recurrent neural nets and problem solutions,” *Int. J. Uncertainty, Fuzziness Knowledge-Based Syst.*, vol. 6, no. 02, pp. 107–116, 1998.

[82] M. Sabri and M. El Hassouni, “A Comparative Study of LSTM and RNN for Photovoltaic Power Forecasting,” in *International Conference on Advanced Technologies for Humanity*, 2021, pp. 265–274.

[83] D. P. Ananthu and K. Neelashetty, “A study of 100kWp PV Plant Output Power Forecasting: A case study,” in *2021 5th International Conference on Computing Methodologies and Communication (ICCMC)*, 2021, pp. 723–728.

[84] K. Cho *et al.*, “Learning phrase representations using RNN encoder-decoder for statistical machine translation,” *arXiv Prepr. arXiv1406.1078*, 2014.

[85] G. Weiss, Y. Goldberg, and E. Yahav, “On the practical computational power of finite precision RNNs for language recognition,” *arXiv Prepr. arXiv1805.04908*, 2018.

[86] M. Hosseini, S. Katragadda, J. Wojtkiewicz, R. Gottumukkala, A. Maida, and T. L. Chambers, “Direct normal irradiance forecasting using multivariate gated recurrent units,” *Energies*, vol. 13, no. 15, p. 3914, 2020.

[87] I. Jebli, F.-Z. Belouadha, M. I. Kabbaj, and A. Tilioua, “Deep learning based models for solar energy prediction,” *Adv. Sci*, vol. 6, pp. 349–355, 2021.

[88] J. He and J. Xu, “Ultra-short-term wind speed forecasting based on support vector machine with combined kernel function and similar data,” *EURASIP J. Wirel. Commun. Netw.*, vol. 2019, no. 1, pp. 1–7, 2019.

[89] F. Gorunescu, *Data Mining: Concepts, models and techniques*, vol. 12. Springer Science & Business Media, 2011.

[90] M. Hossain, S. Mekhilef, and L. Olatomiwa, “Performance evaluation of a stand-alone PV-wind-diesel-battery hybrid system feasible for a large resort center in South China Sea, Malaysia,” *Sustain. cities Soc.*, vol. 28, pp. 358–366, 2017.

[91] H. S. Jang, K. Y. Bae, H.-S. Park, and D. K. Sung, “Solar power prediction based on satellite images and support vector machine,” *IEEE Trans. Sustain. Energy*, vol. 7, no. 3, pp. 1255–1263, 2016.

[92] X. Huang, A. Maier, J. Hornegger, and J. A. K. Suykens, “Indefinite kernels in least squares support vector machines and principal component analysis,” *Appl. Comput. Harmon. Anal.*, vol. 43, no. 1, pp. 162–172, 2017.

[93] H. Tabari, O. Kisi, A. Ezani, and P. H. Talaee, “SVM, ANFIS, regression and climate based models for reference evapotranspiration modeling using limited climatic data in a semi-arid highland environment,” *J. Hydrol.*, vol. 444, pp. 78–89, 2012.

[94] V. H. Quej, J. Almorox, J. A. Arnaldo, and L. Saito, “ANFIS, SVM and ANN soft-computing techniques to estimate daily global solar radiation in a warm sub-humid environment,” *J. Atmos. Solar-Terrestrial Phys.*, vol. 155, pp. 62–70, 2017.

[95] A. Ahmad, Y. Jin, C. Zhu, I. Javed, M. Waqar Akram, and N. A. Buttar, “Support vector machine based prediction of photovoltaic module and power station parameters,” *Int. J. Green Energy*, vol. 17, no. 3, pp. 219–232, 2020.

[96] F. Hamamy and A. M. Omar, “Least square support vector machine technique for short term solar irradiance forecasting,” in *AIP Conference Proceedings*, 2019, vol. 2129, no. 1, p. 20133.

[97] M. Malvoni and N. Hatziargyriou, “One-day ahead PV power forecasts using 3D Wavelet Decomposition,” in *2019 International Conference on Smart Energy Systems and Technologies (SEST)*, 2019, pp. 1–6.

[98] G.-B. Huang, Q.-Y. Zhu, and C.-K. Siew, “Extreme learning machine: theory and applications,” *Neurocomputing*, vol. 70, no. 1–3, pp. 489–501, 2006.

[99] H. C. Leung, C. S. Leung, and E. W. M. Wong, “Fault and noise tolerance in the incremental extreme learning machine,” *IEEE Access*, vol. 7, pp. 155171–155183, 2019.

[100] W.-Y. Deng, Z. Bai, G.-B. Huang, and Q.-H. Zheng, “A fast SVD-Hidden-nodes based extreme learning machine for large-scale data Analytics,” *Neural Networks*, vol. 77, pp. 14–28, 2016.

[101] J. Huang, Z. L. Yu, and Z. Gu, “A clustering method based on extreme learning machine,” *Neurocomputing*, vol. 277, pp. 108–119, 2018.

[102] X. Li, S. He, Z. Wei, and L. Wu, “Improved online sequential extreme learning

machine: a new intelligent evaluation method for AZ-style algorithms," *IEEE Access*, vol. 7, pp. 124891–124901, 2019.

[103] M. Zhang, X. Liu, and Z. Zhang, "A soft sensor for industrial melt index prediction based on evolutionary extreme learning machine," *Chinese J. Chem. Eng.*, vol. 24, no. 8, pp. 1013–1019, 2016.

[104] P. Tang, D. Chen, and Y. Hou, "Entropy method combined with extreme learning machine method for the short-term photovoltaic power generation forecasting," *Chaos, Solitons & Fractals*, vol. 89, pp. 243–248, 2016.

[105] M. Hossain, S. Mekhilef, M. Danesh, L. Olatomiwa, and S. Shamshirband, "Application of extreme learning machine for short term output power forecasting of three grid-connected PV systems," *J. Clean. Prod.*, vol. 167, pp. 395–405, 2017.

[106] F. Neumann and C. Witt, "Bioinspired computation in combinatorial optimization: Algorithms and their computational complexity," in *Proceedings of the 15th annual conference companion on Genetic and evolutionary computation*, 2013, pp. 567–590.

[107] L. Yang and A. Shami, "On hyperparameter optimization of machine learning algorithms: Theory and practice," *Neurocomputing*, vol. 415, pp. 295–316, 2020.

[108] M.-Y. Cho, C.-H. Lee, and J.-M. Chang, "Application of Parallel ANN-PSO to Hourly Solar PV Estimation," 2021.

[109] A. Bao, S. Fei, and M. Zhong, "Short-term solar irradiance forecasting using neural network and genetic algorithm," in *Chinese Intelligent Systems Conference*, 2016, pp. 619–627.

[110] H. T. C. Pedro and C. F. M. Coimbra, "Assessment of forecasting techniques for solar power production with no exogenous inputs," *Sol. Energy*, vol. 86, no. 7, pp. 2017–2028, 2012.

[111] S. Jafarian-Namin, A. Goli, M. Qolipour, A. Mostafaeipour, and A.-M. Golmohammadi, "Forecasting the wind power generation using Box–Jenkins and hybrid artificial intelligence: A case study," *Int. J. Energy Sect. Manag.*, 2019.

[112] X. Wang, D. Luo, and C. Li, "ABC-SVM and PSO-RF Model for Photovoltaic Forecasting Based on Big Data," in *2019 2nd International Conference on Artificial Intelligence and Big Data (ICAIBD)*, 2019, pp. 97–101.

[113] W. VanDeventer *et al.*, "Short-term PV power forecasting using hybrid GASVM technique," *Renew. energy*, vol. 140, pp. 367–379, 2019.

[114] D. Niu, Y. Wang, and D. D. Wu, "Power load forecasting using support vector

machine and ant colony optimization," *Expert Syst. Appl.*, vol. 37, no. 3, pp. 2531–2539, 2010.

[115] M. K. Behera, I. Majumder, and N. Nayak, "Solar photovoltaic power forecasting using optimized modified extreme learning machine technique," *Eng. Sci. Technol. an Int. J.*, vol. 21, no. 3, pp. 428–438, 2018.

[116] I. Mansoury, D. El Bourakadi, A. Yahyaouy, and J. Boumhidi, "Hourly Solar Power Forecasting Using Optimized Extreme Learning Machine," in *International Conference on Digital Technologies and Applications*, 2022, pp. 629–637.

[117] A. Sözen, E. Arcaklioğlu, M. Özalp, and E. G. Kanit, "Use of artificial neural networks for mapping of solar potential in Turkey," *Appl. Energy*, vol. 77, no. 3, pp. 273–286, 2004.

[118] M. Rana, R. Chandra, and V. G. Agelidis, "Cooperative neuro-evolutionary recurrent neural networks for solar power prediction," in *2016 IEEE Congress on Evolutionary Computation (CEC)*, 2016, pp. 4691–4698.

[119] T. Vinothkumar and K. Deeba, "Hybrid wind speed prediction model based on recurrent long short-term memory neural network and support vector machine models," *Soft Comput.*, vol. 24, no. 7, pp. 5345–5355, 2020.

[120] A. Yona, T. Senjyu, T. Funabashi, and C.-H. Kim, "Determination method of insolation prediction with fuzzy and applying neural network for long-term ahead PV power output correction," *IEEE Trans. Sustain. Energy*, vol. 4, no. 2, pp. 527–533, 2013.

[121] Z. Niu, Z. Yu, W. Tang, Q. Wu, and M. Reformat, "Wind power forecasting using attention-based gated recurrent unit network," *Energy*, vol. 196, p. 117081, 2020.

[122] C. Voyant *et al.*, "Machine learning methods for solar radiation forecasting: A review," *Renew. Energy*, vol. 105, pp. 569–582, 2017.

[123] Z.-F. Liu, L.-L. Li, M.-L. Tseng, and M. K. Lim, "Prediction short-term photovoltaic power using improved chicken swarm optimizer-extreme learning machine model," *J. Clean. Prod.*, vol. 248, p. 119272, 2020.

[124] F. Hutter, J. Lücke, and L. Schmidt-Thieme, "Beyond manual tuning of hyperparameters," *KI-Künstliche Intelligenz*, vol. 29, no. 4, pp. 329–337, 2015.

[125] T. Sahdane, B. Azize, A. Laghrabli, R. Benallal, H. Bougharraf, and B. Kabouchi, "High Fill Factor and Conversion Efficiency in Organic Photovoltaic Cells with PEDOT: PSS/C60."

[126] J. Kennedy and R. Eberhart, "Particle swarm optimization," in *Proceedings of ICNN'95-international conference on neural networks*, 1995, vol. 4, pp. 1942–1948.

[127] Z. Chen *et al.*, “The optimization of accuracy and efficiency for multistage precision grinding process with an improved particle swarm optimization algorithm,” *Int. J. Adv. Robot. Syst.*, vol. 17, no. 1, p. 1729881419893508, 2020.

[128] D. Karaboga, “An idea based on honey bee swarm for numerical optimization,” Technical report-tr06, Erciyes university, engineering faculty, computer …, 2005.

[129] D. Karaboga and B. Basturk, “A powerful and efficient algorithm for numerical function optimization: artificial bee colony (ABC) algorithm,” *J. Glob. Optim.*, vol. 39, no. 3, pp. 459–471, 2007.

[130] D. E. Goldberg and K. Deb, “A comparative analysis of selection schemes used in genetic algorithms,” in *Foundations of genetic algorithms*, vol. 1, Elsevier, 1991, pp. 69–93.

RESUME

Ali Kamil was born in Thi Qar, Iraq in 1994. He completed primary and elementary education in Nasiriyah, the center of Thi Qar, southern Iraq. In 2012, he graduated with Diploma in pumps and gas turbines, from the Department of Mechanics, Baghdad Oil Training Institute. In 2018, he graduated from the Mechatronic Department, AL-Khwarizmi College of Engineering, Baghdad University. After that, he worked as an engineer, control and systems maintenance in the Basra Oil Company in the period 2018-2020. In 2020, He took a leave of absence from work to continue his master's education at his own expense in Turkey. He started his master's academic program at Karabuk University, where he completed the courses and passed the Courses required to be eligible to write the dissertation. In 2021, He started the Practical part and his master's thesis research.